Basin Research

IAS EAGE

Basin Research (2018) 1–22, doi: 10.1111/bre.12272

Refining stratigraphy and tectonic history using detrital zircon maximum depositional age: an example from the Cerro Fortaleza Formation, Austral Basin, southern Patagonia

Zachary T. Sickmann,* Theresa M. Schwartz† and Stephan A. Graham*

**Department of Geological Sciences, Stanford University, Stanford, CA, USA*

†*Department of Geology, Allegheny College, Meadville, PA, USA*

ABSTRACT

The north–south trending, Late Cretaceous to modern Magallanes–Austral foreland basin of southernmost Patagonia lacks a unified, radiometric, age-controlled stratigraphic framework. By simplifying the sedimentary fill of the basin to deep-marine, shallow-marine and terrestrial deposits, and combining 13 new U-Pb detrital zircon maximum depositional ages (DZ MDAs) with published DZ MDAs and U-Pb ash ages, we provide the first attempt at a unified, longitudinal stratigraphic framework constrained by radiometric age controls. We divide the foreland basin history into two phases, including (1) an initial Late Cretaceous shoaling upward phase and (2) a Cenozoic phase that overlies a Palaeogene unconformity. New DZ samples from the shallow-marine La Anita Formation, the terrestrial Cerro Fortaleza Formation and several previously unrecognized Cenozoic units provide necessary radiometric age controls for the end of the Late Cretaceous foreland phase and the magnitude of the Palaeogene unconformity in the Austral sector of the basin. These samples show that the La Anita and Cerro Fortaleza Formations have Campanian DZ MDAs, and that overlying Cenozoic strata have Eocene to Miocene DZ MDAs. By filling this data gap, we are able to provide a first attempt at constructing a basinwide, age-controlled stratigraphic framework for the Magallanes–Austral foreland basin. Results show southward progradation of shallow marine and terrestrial environments from the Santonian through the Maastrichtian, as well as a northward increase in the magnitude of the Palaeogene unconformity. Furthermore, our new age data significantly impact the chronology of fossil flora and dinosaur faunas in Patagonia.

INTRODUCTION

The Magallanes–Austral foreland basin (MAB) is the southernmost in the chain of Andean foreland basins that developed during Cretaceous to recent time. The MAB is built on the remnants of the Triassic—Jurassic Rocas Verdes extensional basin, which formed during the extensional separation of Gondwana (Dalziel, 1981; Wilson, 1991; Pankhurst *et al.*, 2000; Fig. 1). The history of the north–south elongate basin can be broadly divided into three phases, including (1) an initial extensional phase (Jurassic to early Cretaceous (Fig. 1b); (2) a Late Cretaceous foreland basin phase characterized by deep-marine depositional environments, which transitioned through time to shallow-marine and coastal environments (Fig. 1b); and (3) a Cenozoic foreland basin phase characterized by terrestrial and shallow-marine environments (Fig. 1b; Biddle *et al.*, 1986; Wilson, 1991). The MAB outcrop belt extends for over 800 km from approximately 48° S to the southern tip of the South American continent (55° S; Fig. 1). The outcrop belt varies in width from <50 km to more than 200 km, and is intersected by an east–west jog in the otherwise north–south oriented political border between Chile and Argentina (at approximately 50.6° S; Fig. 2). The basin is referred to as the Austral Basin in Argentina, and as the Magallanes Basin in Chile. These areas are referred to herein as the 'Austral sector' and 'Magallanes sector' of the MAB (e.g. Fig. 2; Malkowski *et al.*, 2015a,b).

Political boundary division of the basin and outcrop belt has resulted in suites of studies from each area that are not well unified with regard to stratigraphic age and nomenclature, stratigraphic framework and interpretations of basin evolution for the entire foreland basin fill. The

Correspondence: Zachary T. Sickmann, Department of Geological Sciences, Stanford University, Stanford, CA 94305, USA. E-mail: zsickman@stanford.edu

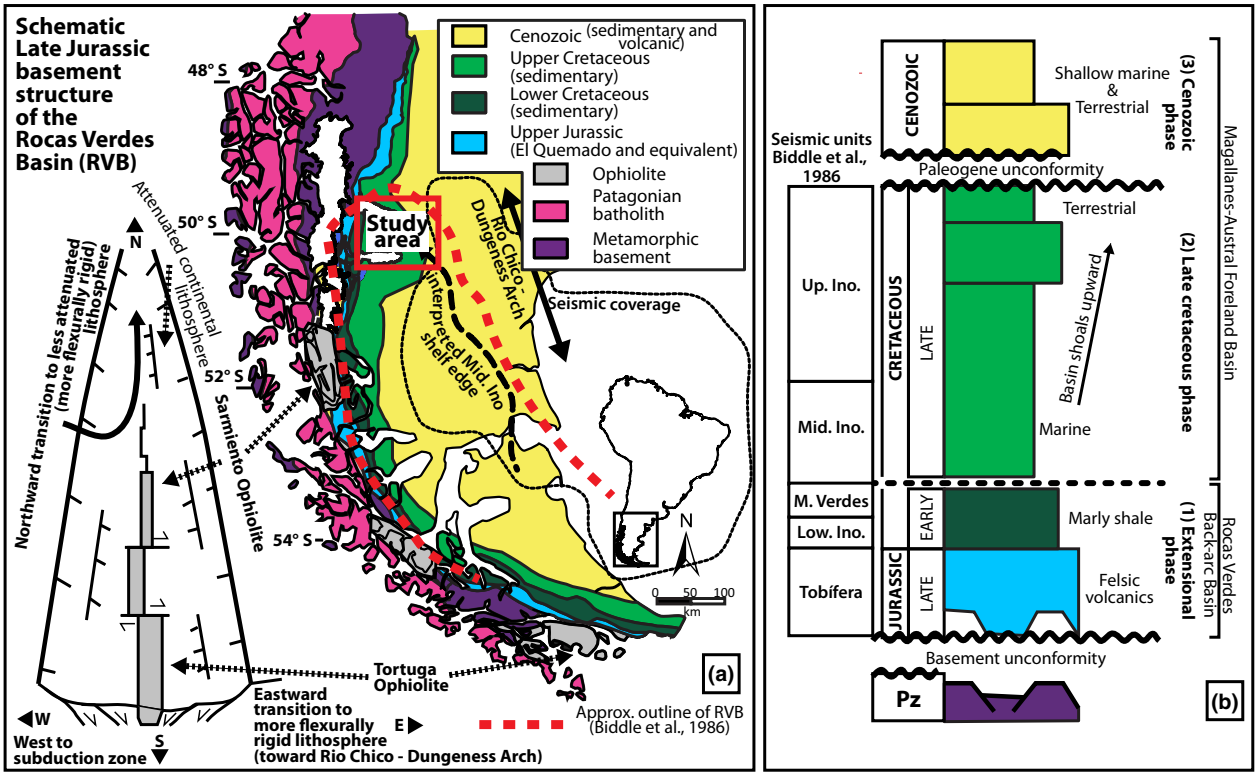

Fig. 1. (a) Overview map of southern South America showing the location of the Magallanes–Austral Foreland Basin (MAB; modified from Biddle *et al.*, 1986); Wilson, 1991). Seismic coverage outline represents the extent of subsurface data presented by Biddle *et al.* (1986) and Sachse *et al.* (2015). Dashed line with arrow represents the interpreted Cenomanian shelf edge and its projection through the study area from Biddle *et al.* (1986). The inset to the left of the map illustrates the northward 'unzipping' structure of predecessor RVB basin that underlies the MAB (after de Wit & Stern, 1981; Ramos *et al.*, 1982). Arrows show where ophiolite sequences shown schematically in the inset are in the basin providing spatial reference for the RVB basement configuration. (b) Simplified stratigraphy of the MAB shown schematically (after Biddle *et al.*, 1986; Fosdick *et al.*, 2011). Unit widths correspond to relative resistance in outcrop profile. Subsurface units are after Biddle *et al.* (1986). Low. Ino.: lower Inocermaus; M. Verdes: Margas Verdes; Mid. Ino.: middle Inoceramus; Up. Ino.: upper Inoceramus.

myriad of complications that contribute to this include variations in nomenclature, mapping and proposed depositional ages for equivalent stratigraphic intervals (Fig. 3; Fig. S1 and Appendix S1). This is compounded by a paucity of absolute age control, and the conflicting nature of that which exists, in the northern part of the basin (e.g. Varela *et al.*, 2012a; Malkowski *et al.*, 2015a, 2017). This has led to difficulty in producing a unified stratigraphic framework for the entire MAB fill, extending north to south across the Argentina–Chile border.

In order to alleviate the confusion associated with such issues, we use a compilation of new and published mapping to divide MAB foreland deposits into three broad categories, including (1) dominantly deep-marine deposits, (2) dominantly shallow marine deposits and (3) dominantly terrestrial deposits (Fig. 2). Using these simplified lithologic/palaeoenvironmental delineations, we adopt published radiometric age data from igneous and detrital samples and couple them with new detrital zircon maximum depositional ages (DZ MDAs) to provide the first

Fig. 2. (a) Map of the MAB showing the modern extent of lithostratigraphic units and the locations of zircon samples from this and previous studies (e.g. Fildani *et al.*, 2003; Romans *et al.*, 2010; Bernhardt *et al.*, 2011; Fosdick *et al.*, 2011, 2014, 2015; Malkowski *et al.*, 2015a, 2017; Schwartz *et al.*, 2016). Phase 1 deposits are divided by lithology into felsic volcanic rocks and marly shale. Phases 2 and 3 deposits are divided by dominant depositional environment into deep-marine, shallow-marine and terrestrial deposits. Base mapping is from Fosdick *et al.* (2011, 2014), Giacosa *et al.* (2012), Ghiglione *et al.* (2014), Malkowski *et al.* (2015a), Schwartz & Graham (2015) and this study (SAR: Lago Sarmiento, TOR: Lago Toro). (b) Simplified stratigraphic columns from different parts of the basin that show depositional environment and variable nomenclature across the basin. Austral sector nomenclature is after Arbe & Hechem (1984) and this study. Magallanes sector nomenclature is after Wilson (1991). White dashed line delineates phase 1 stratigraphy from phase 2.

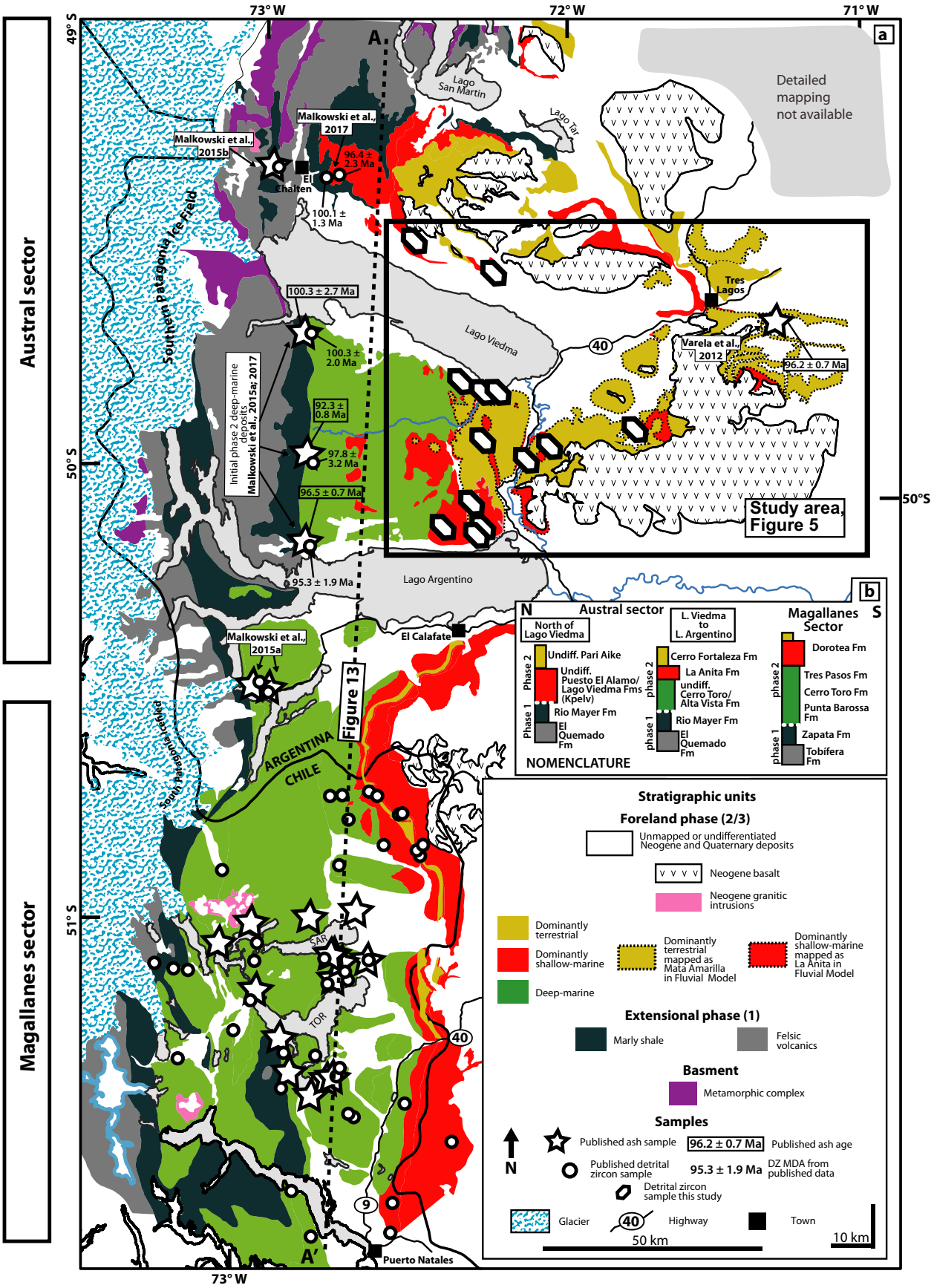

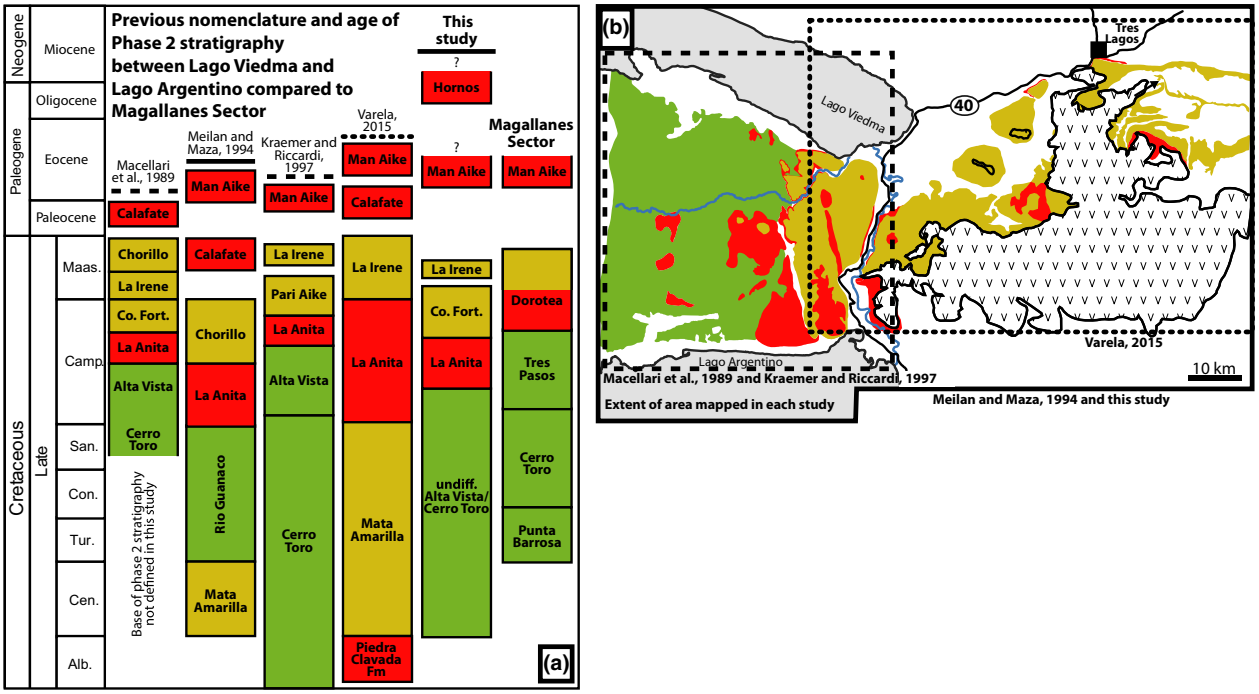

Fig. 3. (a) Summary of previously used nomenclature and chronostratigraphy of the area between Lago Viedma and Lago Argentino. Cerro Fortaleza is abbreviated to Co. Fort. Note that all units shown here were given formation status by these authors. We prefer not to delineate the La Irene and Cerro Hornos sandstone (abbreviated Hornos here) as Formations at this time. Note that the Pari Aike Formation of Kraemer & Riccardi (1997) is not correlative with what we here define as 'undifferentiated Pari Aike Formation' north of Lago Viedma. See Fig. S1 and Appendix S1 for a more detailed explanation of nomenclature. Magallanes stratigraphy is compiled from Bernhardt *et al.* (2011) and Daniels *et al.* (2017). (b) Area mapped by each study. Note that for Meilan & Maza (1994), mapping extends beyond the boundaries of this figure. Colour scheme for both a and b follows Fig. 2. See Fig. 6 for more detailed spatial references (Lat/Long) for the study area.

unified, radiometrically controlled, stratigraphic correlation for the entire upper Cretaceous to lower Cenozoic foreland basin fill between 49° S and 51.5° S. Our correlations show that (1) the initial Late Cretaceous foreland was marine throughout this portion of the MAB and (2) the cessation of marine conditions, which represents the end of the Late Cretaceous foreland phase, signalled southward progradation of deltaic deposits across the basin beginning in Campanian time. Additionally, our data put new constraints on the regional unconformity that separates the Late Cretaceous (phase 2) and Cenozoic (phase 3) phases of the basin fill, and indicate that the time represented by the unconformity decreases significantly from north to south. This framework provides the foundation for more detailed studies across the Austral sector of the basin and broad depositional context for the detailed work that has already been done in the Magallanes sector.

BASIN HISTORY

As part of southwestern Gondwana, present-day southern Patagonia was affected by extensional tectonism in Early Jurassic time (phase 1; Fig. 1). Concurrently, an offshore subduction zone and associated magmatic arc (represented today by the Patagonia batholith) were located to the west (Fig. 1b). Voluminous episodes of bimodal continental volcanism record the extension phase (Pankhurst *et al.*, 2000). Extension progressed northward from the southern end of Patagonia, and was sufficient to create a series of ophiolite complexes south of 51° S (Fig. 1; de Wit & Stern, 1981). Silicic volcanism, recorded by the Chon Aike large igneous province, accompanied extension from *ca.* 190 to 150 Ma across the Patagonia region (Pankhurst *et al.*, 2000). In the MAB, volcanism is recorded by the Tobífera and El Quemado Formations, which range in age from 154 to 147 Ma (Malkowski *et al.*, 2015b). Geochemical data from the ophiolite sequences and geochronologic data from rift-associated volcanic rocks suggest that rifting continued longer and extended further in the south than the north (Fig. 1; de Wit & Stern, 1981; Caldéron *et al.*, 2013; Malkowski *et al.*, 2015b). The diachronous extension created the Rocas Verdes back-arc basin (RVB), a north–south elongate basin floored by oceanic crust in the south and attenuated continental crust in the north, with a similar westward and eastward decrease in the degree of attenuation, away from the locus of rifting (Fig. 1a, inset). The tectonic

regime transitioned from extensional to compressional at approximately 115 Ma, initiating phase 2 of the basin history with the formation of the MAB on top of the RVB (Wilson, 1991; Ghiglione *et al.*, 2015; Malkowski *et al.*, 2015a).

The extensional structures of the predecessor RVB fundamentally influenced the initial construction of the MAB (Wilson, 1991; Romans *et al.*, 2010). The north to south increase in basement attenuation resulted in a deeply subsided foredeep in the southern part of the basin (Magallanes sector), which was loaded by obducted, dense, ophiolitic crust (Fosdick *et al.*, 2014). Loading of the attenuated lithosphere was modelled by Fosdick *et al.* (2014) who showed that this configuration generated a deeply subsided foredeep with pinned and subdued forebulge and backbulge areas that do not appreciably migrate through time. To the north, the foreland was floored by less attenuated, more flexurally rigid lithosphere (Ramos *et al.*, 1982). The north to south variation in basement attenuation and loading also generated a southward-dipping depositional gradient with the underfilled, deeply subsided Magallanes sector attaining water depths up to 2000 m (Natland *et al.*, 1974). This is consistent with the idea that a thinner elastic lithosphere with lower flexural rigidity will subside more deeply than a more rigid, thicker elastic lithosphere under a topographic load (summarized for the MAB in Fosdick *et al.*, 2014). The MAB progressively shifted to compression southward, in the opposite direction that the RVB opened. Initial foreland sedimentation began in the northernmost Austral sector as early as 115 Ma (Ghiglione *et al.*, 2015; Malkowski *et al.*, 2015a) and progressed south to the Magallanes sector by 93 Ma (Fildani *et al.*, 2003; Bernhardt *et al.*, 2011). Palaeocurrent and provenance data from the foreland basin fill show that sediment transport was dominantly longitudinal, and mean palaeodispersal was north to south along the axis of the basin following delivery of sediment to the basin by transverse depositional systems (Bernhardt *et al.*, 2011; Malkowski *et al.*, 2015a, 2017). After initial foreland flexural subsidence, the basin shoaled through the Late Cretaceous (Wilson, 1991). Continued thrust belt evolution led to phase 3 of the basin (Fig. 1b) (Fosdick *et al.*, 2015). The initiation of the phase 3 is marked by a regional Palaeogene unconformity that separates Cretaceous and Cenozoic deposits across the basin. Cenozoic deposition resumed diachronously across the basin in shallow marine and terrestrial environments.

PREVIOUS WORK

Nomenclature

A brief explanation of existing stratigraphic nomenclature is required, particularly in the Austral sector for which a unified naming scheme has not been established. To simplify regional lithostratigraphic trends, we divide the MAB stratigraphy into three broad categories based on dominant depositional environments (deep marine, shallow marine and terrestrial; Fig. 2). Each of the three bins encompasses multiple stratigraphic units. An alternate version of Fig. 2 that subdivides map units by their formal formation/unit names and includes east–west oriented schematic cross-sections is provided in Fig. S1. This is accompanied by a synthesis of information for each map unit (Appendix S1), which includes lithologic characteristics, age controls, naming schemes and brief synopses of previous work that has been done for each unit. Figure 3 summarizes the nomenclature that has recently been used in the study area.

For the remainder of the text, we simplify formation names that have been used in the Austral sector as follows (see Figs 2a and 4): (1) All deep-marine deposits in the Austral sector are herein referred to as 'undifferentiated Cerro Toro/Alta Vista Formation' (Fig. 2b); (2) shallow-marine deposits that outcrop north of Lago Viedma are referred to as 'undifferentiated Lago Viedma/Puesto El Alamo Formation' (Kpelv; Fig. 2b); (3) shallow-marine deposits that outcrop between Lago Argentino and Lago Viedma are referred to as 'La Anita Formation'; (4) terrestrial deposits that outcrop north of Lago Viedma are informally referred to as 'undifferentiated Pari Aike Formation' (these rocks are differentiated from the Cerro Fortaleza Formation because they are likely not age equivalent); and (5) terrestrial deposits that outcrop between Lago Viedma and Lago Argentino and to the east past Tres Lagos are referred to as 'Cerro Fortaleza Formation'. This final delineation, 'Cerro Fortaleza Formation', includes rocks that have sometimes been named 'Mata Amarilla Formation' (Figs 2 and 3), and have previously been assigned a Cenomanian age (e.g. Riccardi & Rolleri, 1980; Varela *et al.*, 2012a). Areas that were previously mapped as Mata Amarilla Formation are outlined with dashed lines in Figs 2 and 4. In some places in the Austral sector, there is a tan fluvial sandstone unit between the Cerro Fortaleza Formation and overlying Cenozoic strata. We refer to this unit as the 'La Irene sandstone', after the La Irene Formation that was defined by Macellari *et al.* (1989). However, we prefer not to give the unit formation status, as discussed in Appendix S1.

For the Magallanes sector, we employ the conventionally established naming scheme that includes the Punta Barrosa, Cerro Toro and Tres Pasos formations for deep-marine deposits and the Dorotea Formation for shallow-marine to terrestrial deposits (after Wilson, 1991) (Fig. 2b). Cenozoic units of Eocene age or probable Eocene age are called 'Man Aike Formation'. All other Cenozoic units in the Magallanes sector are undifferentiated in this study.

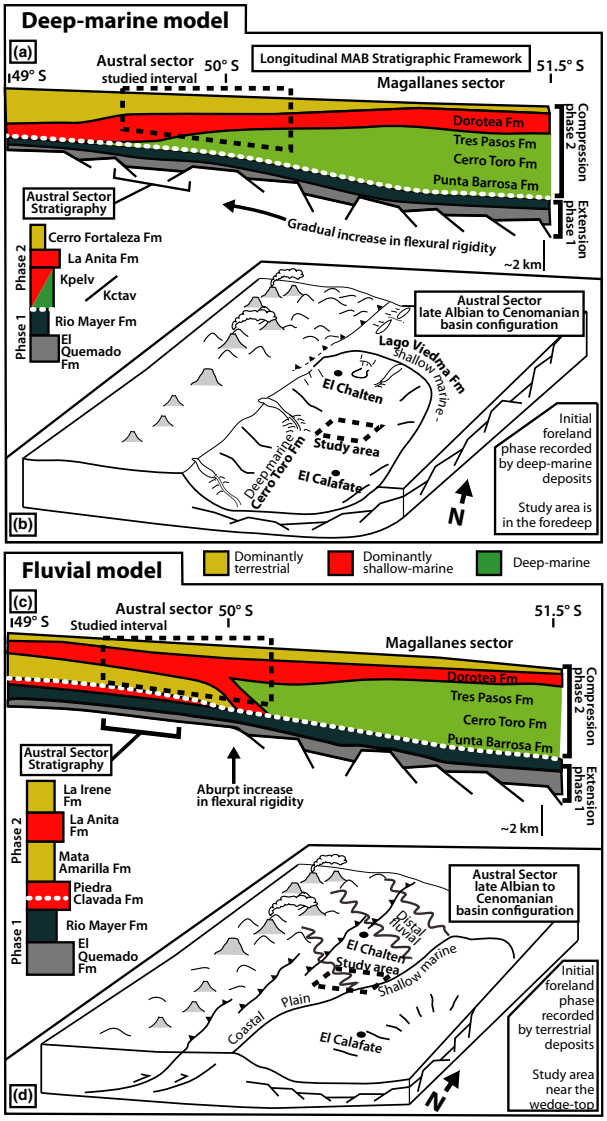

Fig. 4. Conceptual basin models and longitudinal stratigraphic frameworks of the two end-member basin models during the earliest foreland phase. (a) 'Deep-marine' model after Arbe & Hechem (1984) and others (Kpelv: undifferentiated Lago Viedma and Puesto El Alamo Formations; Kctav: undifferentiated Cerro Toro and Alta Vista Formations). (b) 'Fluvial' model after Varela *et al.* (2012a,b, 2013). The towns of El Calafate and El Chalten are displayed to give spatial reference. The locations of these towns are on Fig. 2. White dashed lines represent delineations between phase 1 and phase 2 stratigraphy.

Existing stratigraphic frameworks

The stratigraphic framework and chronology of phase 1 (RVB) is relatively well established, aided by abundant dateable volcanic material (e.g. Pankhurst *et al.*, 2000; Stern & De Wit, 2003; Malkowski *et al.*, 2015b). The most fundamental questions regarding the longitudinal stratigraphic framework of the foreland phases 2 and 3 of the MAB are: (1) What are the ages and depositional environments associated with the initial foreland phase 2 deposits across the basin (Fig. 1b)? (2) When was the cessation of marine deposition and the transition to terrestrial deposition across the basin during the Late Cretaceous foreland phase 2 (Fig. 1b)? (3) How much time is represented by the Palaeogene unconformity that occurs at the start of phase 3, and how does this vary across the basin (Fig. 1b)? Extensive radiometric age control from the Magallanes sector (Fig. 2) has provided a robust stratigraphic framework that addresses these questions in the southern half of the basin system (e.g. Fig. 2a; Bernhardt *et al.*, 2011; Daniels *et al.*, 2017). The Austral sector of the basin, however, lacks extensive age control (Fig. 2a).

Early work that proposed a longitudinal stratigraphic framework for the basin suggested that the initial foreland phase 2 deep-water environments that existed in the Magallanes sector continued north into the Austral sector (e.g. Arbe & Hechem, 1984; Riccardi & Aguirre-Uretta, 1988). The Austral deep-marine system was considered to grade laterally into age-equivalent shallow-marine strata somewhere north of Lago Viedma (Fig. 2; Riccardi & Rolleri, 1980; Arbe, 2002), and was also thought to shoal upward through Late Cretaceous time in a similar fashion to the Magallanes sector (Macellari *et al.*, 1989; Arbe, 2002). This framework was based on field observations and regional biostratigraphic delineations, and prevailed as the dominant model until the first radiometric age data from the Austral sector was published by Varela *et al.* (2012a).

Varela *et al.* (2012a,b) published a Cenomanian (96.2 ± 0.7 Ma) U-Pb age from an ash near Tres Lagos (Figs 2 and 3), which was collected from terrestrial deposits that are referred to by those authors as the Mata Amarilla Formation. Varela *et al.* (2012a,b) correlated these terrestrial deposits as far south as the north shore of Lago Argentino (Figs 2 and 3). They noted eastward-directed palaeocurrent indicators and sandstone provenance that were consistent with derivation from the southern Andean orogen located to the west, and ultimately interpreted the deposits to represent a Cenomanian, southeast-prograding fluvial system across the Austral sector. Their correlation led to a series of attempts to explain the presence of Cenomanian terrestrial deposits so close to Cenomanian deep-marine deposits in the adjacent Magallanes sector. Based on the differences in basin history interpretations that are based on original field observations (Arbe & Hechem, 1984; Riccardi & Aguirre-Uretta, 1988) and more recent radiometric dating (Varela *et al.*, 2012a), stratigraphic models for the Austral sector can be divided into two end members (Figs 2 and 3).

We refer to the first end-member model as the 'deep-marine model'. This model is based on original geologic mapping of the Austral sector which suggests that Cenomanian deep-marine environments extended well into the Austral sector, with a gradual northward transition into

time-equivalent shallow-marine and terrestrial environments (Fig. 4a; Arbe & Hechem, 1984). We refer to the second end-member model as the 'fluvial model' (Fig. 2b; after Varela *et al.*, 2012a, 2013). This model suggests that foreland sedimentation initiated in the Austral sector with terrestrial environments that abruptly transition southward into the deep-marine environments of the Magallanes sector (Fig. 4b). Importantly, the fluvial model does not acknowledge the existence of deep-marine facies in the Austral sector of the MAB.

Even within the parameters of previously existing data, the fluvial model suffers from several inconsistencies. The most fundamental of these inconsistencies is the presence of Cenomanian deep-marine strata located immediately west of terrestrial deposits that have been defined as Cenomanian and display eastward palaeodispersal (e.g. Fig. 2; Varela *et al.*, 2013). Even before recent U-Pb zircon data established a Cenomanian age for the deep-marine succession (Malkowski *et al.*, 2015a), regional biostratigraphic and stratal relationships had suggested these rocks were part of a Cenomanian deep-marine depositional system (e.g. Kraemer & Riccardi, 1997; Arbe, 2002). Additionally, seismic data suggest that deposits representing a Cenomanian Austral sector shelf-edge projects beneath the study area in the subsurface (Fig. 1a; Biddle *et al.*, 1986; Sachse *et al.*, 2015).

Despite these inconsistencies, the Cenomanian tuff age from the terrestrial deposits east of Tres Lagos (Varela *et al.*, 2012a) has remained the only radiometric age control for the eastern part of the Austral sector. Attempts to conceptually reconcile the stratigraphic inconsistencies have focused on explanations that invoke an abrupt transition in the flexural rigidity and elastic thickness of the lithosphere that underlies the MAB between the Austral and Magallanes sectors (e.g. Varela *et al.*, 2013; Fig. 2b). Antecedent structures have been demonstrated to lead to lateral variability in lithospheric flexural rigidity and the associated degree of flexural subsidence in foreland basins (e.g. Desegaulx *et al.*, 1990; Waschbusch & Royden, 1992). However, the north to south transition in flexural rigidity required for the Austral sector to behave as an overfilled foreland dominated by terrestrial depositional environments (by definition, above sea level) and the Magallanes sector to be an underfilled, deeply subsided foredeep dominated by deep-marine depositional environments (with water depths up to 2000 m) during the Cenomanian would be extremely abrupt (<10 km; Fig. 4). Such an interpretation places the purported Cenomanian terrestrial deposits of the Austral sector in a wedge-top setting of the foreland basin complex (cf. Decelles & Giles, 1996), with an abrupt transition southward into the foredeep of the Magallanes sector that was built on more attenuated basement (e.g. Varela *et al.*, 2013). The wedge-top interpretation may explain the close proximity of Cenomanian terrestrial and deep-marine deposits in the Austral and Magallanes sectors, but it fails to explain the presence of Cenomanian deep-marine deposits that are located immediately west of the terrestrial deposits (e.g. Fig. 2) and also omits a foredeep phase of deposition in the Austral sector that would precede the formation of a wedge top (e.g. Decelles & Giles, 1996). Additionally, there is no evidence that the strata were deposited atop actively deforming structures during the Cretaceous. The complicated and often convoluted basin interpretations associated with the 'fluvial model' arise entirely from attempts to explain assumed Cenomanian-aged terrestrial deposits between Lago Vieda and Lago Argentino that sit so close to contemporaneous deep-marine deposits. If the Cenomanian age assignment for terrestrial deposits between Lago Viedma and Lago Argentino can be demonstrated to be incorrect, the remainder of the stratigraphic framework of the basin and interpreted basement rheology fall into place much more simply.

Thirteen detrital zircon samples and new mapping from this study fill the east–west gap in radiometric age control in the region between data presented by Malkowski *et al.*, 2017; Fig. 2a) and Varela *et al.* (2012a,b; Fig. 2a), and provide a multi-sample validation (or invalidation) of the purported Cenomanian age for terrestrial stratigraphy defined in the fluvial model (Figs 2 and 4). Our results are combined with previously published detrital and igneous zircon samples to provide a basinwide stratigraphic framework. Although this study provides the first age control for phase 3 strata in this area, these units remain poorly defined in terms of lithofacies and detailed depositional environment interpretations. Existing literature (e.g. Macellari *et al.*, 1989) suggests that the Cenozoic strata are dominantly shallow marine.

Significance of stratigraphic frameworks with regard to palaeontology

The Austral sector terrestrial deposits, which are of disputed age, host a rich assemblage of Cretaceous vertebrate and macrofloral fossils, including the most complete Titanosaur specimen known to date (Fig. 5; Lacovara *et al.*, 2014). Although the palaeontology community has generally preferred a Campanian to Maastrichtian age assignment for the fossiliferous units (Fig. 5; consistent with the deep-marine model framework for phase 2), several palaeontological studies have applied a Cenomanian to Santonian age based on use of the fluvial model framework (e.g. Fig. 5). Using this older age, Martinez *et al.* (2017) define a new cycad genus and species (*Zamuneria amyla*) and O'Gorman & Varela (2010) define a plesiosaur (*Polyptychodon patagonicus*) as the oldest known Late Cretaceous specimens. However, of greatest importance is the refining of the age of the Theropod specimen *Orkoraptor burkei* (Novas *et al.*, 2008), which was later placed

within the Megaraptoridae clade of the Allosauroidea superfamily (allosauroids) by Benson *et al.* (2010). This specimen was discovered at Cerro Hornos (Fig. 5) and was first described by Novas *et al.* (2008), who originally assigned it a Maastrichtian age, making it the youngest known allosauroid specimen ever discovered (Benson *et al.*, 2010). This age was subsequently reassigned as Cenomanian to Santonian by Novas *et al.* (2013) based on the work of O'Gorman & Varela (2010) who employed the fluvial model age for the unit (Fig. 5). This Cenomanian to Santonian age for the Theropod has subsequently been applied to Gondwana vertebrate biostratigraphy in basins as far as the Bauru Basin in Brazil (Menegazzo *et al.*, 2016). The existence of two ages for these deposits has required palaeontologists to continue to acknowledge the 30 Myr range of possible ages, making definitive placement of fossil discoveries in the context of Gondwanan vertebrate evolution difficult.

METHODS

Sedimentology and stratigraphy

New sedimentological observations, stratigraphic descriptions and geologic mapping for this study was focused on providing context for DZ samples from terrestrial and shallow-marine deposits that are of disputed age (Fig. 5). Three new regional stratigraphic sections were measured at locations 1, 2 and 3 on Fig. 5, and new sections are combined with the published sections of Varela (2015) at locations 4 and 5 (Fig. 5) to create a composite section of the transition from shallow marine to terrestrial deposition and the overlying Cenozoic strata (Fig. 6). Observations from these sections were then used to remap the area between Lago Viedma and Lago Argentino east to Tres Lagos (Fig. 5). We employ the published mapping of Giacosa *et al.* (2012) for the area north of Lago Viedma and the mapping of Ghiglione *et al.* (2014), Malkowski *et al.* (2015a), Fosdick *et al.* (2011, 2014) and Schwartz & Graham (2015) for the Magallanes sector (Figs 2 and 4).

Detrital zircon analyses

Zircon separates were collected from 2 to 3 kg samples of medium-grained sandstone using standard separation procedures (e.g. Schwartz *et al.*, 2016). Detrital zircon grains from 12 of the samples were analysed for U-Pb ages at the Arizona LaserChron Center using LA-ICP-MS on both the Nu (single collector) and Element2 (multicollector) machines. Between 100 and 300 individual grains were analysed per sample. One sample, SM-9, was analysed on the single collector LA-ICP-MS at the University of California Santa Cruz (UCSC). Data reduction for samples analysed at the Arizona LaserChron Center followed the methodologies of Gehrels *et al.* (2008) and Gehrels & Pecha (2014). U-Pb results were filtered using the following criteria: min $^{206}Pb/^{204}Pb = 200$, max discordance = 20% (Element2); 30% (Nu), max reverse discordance = 5%. Less than 5% of the total data was excluded by these filters. All ages used in maximum depositional age calculations were calculated using the $^{206}Pb/^{238}U$ age, as is conventional for grains younger than 900 Ma (Gehrels *et al.*, 2008). Data reduction for sample SM-9 that was analysed at UCSC followed the methodologies outlined by Sharman *et al.* (2013).

Detrital zircon MDA calculations

Ages calculated from the youngest zircon U-Pb radiometric age dates from detrital samples provide a maximum depositional age. This lower age bound is determined under the assumption that sedimentary deposits cannot be older than the youngest crystallization ages of their source rocks, but can be indeterminately younger. For the purposes of this study, we interpret DZ MDAs to be close approximations of true depositional age for two reasons: (1) the Magallanes–Austral Foreland Basin sits in the retroarc position of a highly active magmatic arc (Hervé *et al.*, 2007) and (2) such settings in general (e.g. Dickinson & Gehrels, 2009; Cawood *et al.*, 2012), and this basin specifically (e.g. Fildani *et al.*, 2003; Bernhardt *et al.*, 2011; Malkowski *et al.*, 2015a; Schwartz *et al.*, 2016) have been shown to produce DZ MDAs that accurately (within 5 Ma) mirror depositional ages that were determined through biostratigraphy, strontium isotope stratigraphy and/or volcanic ash U-Pb geochronology.

The statistical methods for calculating maximum depositional age from a suite of individual detrital zircon analyses range from the use of the single youngest grain analysed to more robust statistical treatments involving multiple grains. We employ three methods here following Dickinson & Gehrels (2009) (Table 1). In ascending order of statistical rigor, they are (1) the age of the youngest single grain (YSG; least rigorous), (2) the weighted mean of the youngest cluster of grains that overlap within 1σ error with a minimum of two overlapping grains (YC1σ) and (3) the weighted mean of the youngest cluster of grains that overlap within 2σ error with a minimum of three overlapping grains (YC2σ; most rigorous). For the purposes of primary geologic interpretation, we employ the YC1σ age except in the case of sample CF-1c which does not yield two overlapping young ages (Table 1). For sample CF-1c, we use the YSG age, but recognize that the age is not as robust as other analyses.

We employ the YC1σ age for primary geologic interpretation here for two reasons: (1) This age has been shown to underestimate the true depositional age in <5%

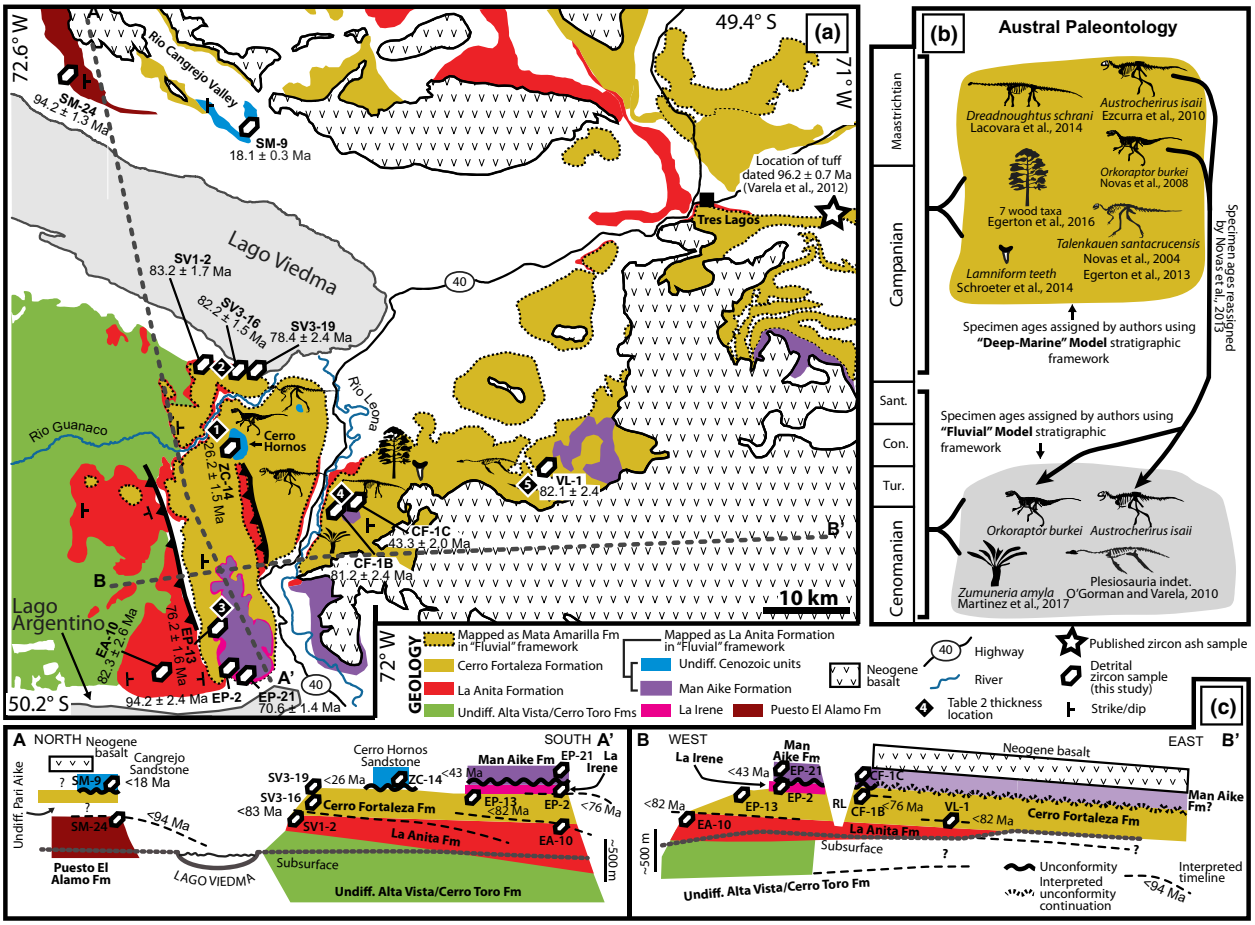

Fig. 5. (a) Simplified study area map showing new geologic mapping from this study between Lago Viedma, Lago Argentino and Tres Lagos. The map displays the location of new geochronology samples from this study, as well as the locations of major palaeontological sites. Mapping from north of Lago Viedma is modified from Giacosa *et al.* (2012) and Meilan & Maza (1994). Mapping east of Tres Lagos is modified from Varela *et al.* (2012a,b). The colour scheme of green (deep marine), red (shallow marine) and yellow (terrestrial) is followed up for the phase 2 stratigraphy between the lakes and correlatives to the north and east with specific formation names assigned in the legend. New colours are given to distinguish other units. (b) Summary of significant Austral sector palaeontological discoveries and their temporal relationships to the two end-member stratigraphic models. (c) Schematic cross-sections of Austral stratigraphy showing new detrital zircon maximum depositional ages. Note that proposed timelines dip from north to south in cross-section A-A', which is in accordance with the general trend of north to south sediment transport and depositional system progradation in the MAB (e.g. Wilson, 1991; Romans *et al.*, 2010; Malkowski *et al.*, 2015a, 2017). Cross-section is schematic and does not follow surface topography in detail to provide room for interpretation. Latitude and longitude numbers refer to the lines of the bounding box.

of samples (e.g. Dickinson & Gehrels, 2009); and (2) the YC1σ age is identical to, or within 2% of, the YC2σ for half the samples from which both statistics were calculable (Table 1). We report the YC2σ for all samples for comparison as the most conservative approximation of maximum depositional age (Table 1).

RESULTS

Sedimentology and stratigraphy

New field observations broadly agree with published lithofacies assemblages and depositional environment interpretations for the phases 2 and 3 shallow-marine and terrestrial deposits that exist between Lago Viedma, Lago Argentino and Tres Lagos (summarized in Fig. 6) (after Macellari *et al.*, 1989; Kraemer & Riccardi, 1997). Shallow-marine, sandstone-dominated lithofacies characterized by laterally continuous, cross-bedded and planar-laminated sand bodies transition up-section to lenticular sandstones and fining upward successions of sandstone and mudstone with abundant palaeosol horizons (Fig. 6). Measured sections indicate that the transition from shallow-marine to terrestrial deposits is conformable, consistent with observations of Macellari *et al.* (1989), Kraemer & Riccardi (1997) and Arbe (2002), and is characterized by an up-section decline and eventual loss of marine fossils including bivalves,

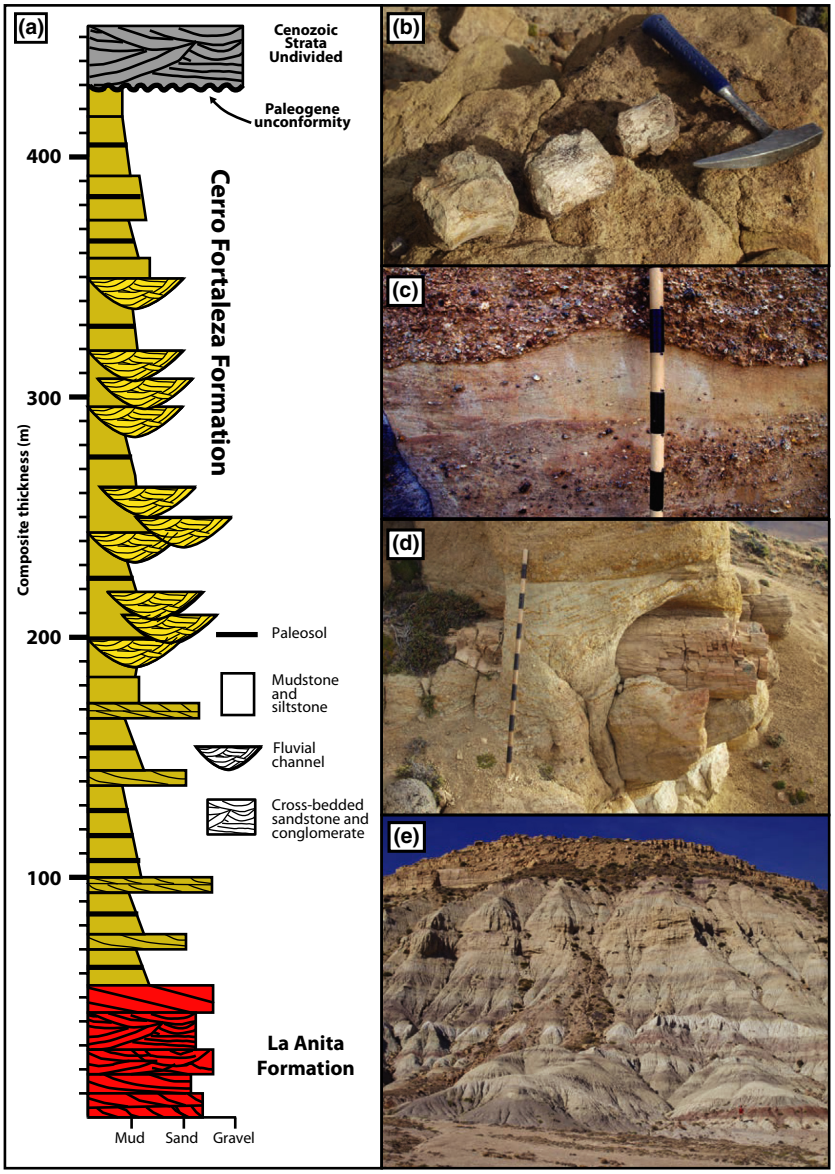

Fig. 6. Summarized phase 2 stratigraphy displayed schematically from between Lago Argentino, Lago Viedma and Tres Lagos (e.g. Fig. 5). (a) Composite stratigraphic section for the upper La Anita Formation (red), the Cerro Fortaleza Formation (yellow) and oldest Cenozoic stratigraphy above the Palaeogene unconformity (grey). (b) Field photo of dinosaur vertebrae common to the Cerro Fortaleza Formation; hammer is 30 cm long. (c) Field photo of lenticular gravel and cross-bedded sandstone common to the coarser intervals of the Cerro Fortaleza Formation; Jacob staff intervals are 10 cm long. (d) Field photo of a large petrified log that is encased in cross-stratified sandstone common in the Cerro Fortaleza Formation; Jacob staff is 1.5 m. (e) Field photo of the colour banding and 'badlands' appearance of the Cerro Fortaleza Formation (outcrop is approximately 200 m high; the upper tan sandstone is the La Irene sandstone).

shark teeth and gastropods, as well as marine trace fossils including *Rhizocorallium*, *Ophiomorpha* and *Skolithos*. Concurrent with the loss of these marine indicators is the appearance of large petrified logs and large vertebrate fossils (Fig. 6). The unconformity that represents the transition from basin phase 2 to basin phase 3 truncates the terrestrial deposits (Fig. 6). Where preserved, the unconformity is the boundary between multicoloured, badlands-forming deposits and dark brown to green, ledge-forming sandstone (Figs 5 and 6). The overlying sandstone deposits commonly contain marine trace fossils and body fossils including oysters, corals and bryozoans (Fig. 6).

North of Lago Viedma shallow-marine units dip eastward into the subsurface in the vicinity of sample SM-24 (Figs 5 and 8). To the east of this, phase 2 upper Cretaceous foreland deposits are poorly constrained in terms of age and lithofacies. Published mapping shows both shallow marine and terrestrial deposits extending east towards Tres Lagos, but a detailed stratigraphy has not yet been fully defined. The Palaeogene unconformity is recognized north of Lago Viedma for the first time in this study. Cenozoic strata are exposed sporadically through the southern part of the Rio Cangrejo Valley (Fig. 5). These deposits consist of coarse-grained, cross-bedded, brown sandstone with abundant oyster fragments (Fig. 7e, f, g). Poor exposure of the Cenozoic units prevents a detailed account of their stratigraphic relationship with underlying Cretaceous strata (Table 2).

Stratigraphic correlations and mapping

Stratigraphic correlations in the western part of the study area, between Lago Viedma and Lago Argentino,

Table 1. Summary of detrital zircon maximum depositional age calculations for all new samples presented in this study. Coordinates are in WGS84.

Sample name	Youngest single grain (Ma ± 1σ)	Youngest overlapping cluster within 1σ error			Youngest overlapping cluster within 2σ error			Preferred MDA	Type	Sample location	
		YC1σ (2+) (Ma ± 2σ)	MSWD	Analyses included	YC2 (Ma ± 2σ)	MSWD	Analyses included			Y	X
SM-9	17.4 ± 0.6	18.1 ± 0.3	0.29	17	18.6 ± 0.2	1.05	32	18.1 ± 0.3	YC1σ(2+)	−49.51523	−72.30791
ZC-14	24.5 ± 1.4	26.2 ± 1.5	2.2	2	N/A	N/A	N/A	26.2 ± 1.5	YC1σ(2+)	−49.87289	−72.22342
CF-1c	43.3 ± 2.0	N/A	N/A	N/A	N/A	N/A	N/A	43.3 ± 2.0	YSG	−49.94261	−72.02241
EP-21	69.1 ± 2.3	70.6 ± 1.4	0.29	8	70.6 ± 1.4	0.29	8	70.6 ± 1.4	YC1σ(2+)	−50.11834	−72.20348
EP-13	74.8 ± 1.7	76.2 ± 1.6	0.21	5	79.7 ± 0.67	1.09	33	76.2 ± 1.6	YC1σ(2+)	−50.05668	−72.23875
VL-1	80.1 ± 2.2	82.1 ± 2.4	0.51	5	85.4 ± 1.2	1.07	16	82.1 ± 2.4	YC1σ(2+)	−49.88539	−71.70526
CF-1b	80.9 ± 2.2	81.2 ± 3.5	0.046	4	84.1 ± 1.2	0.51	10	81.2 ± 3.5	YC1σ(2+)	−49.94113	−72.02663
SV3-19	77.9 ± 2.0	78.4 ± 2.4	0.081	2	82.75 ± 0.85	1.03	18	78.4 ± 2.4	YC1σ(2+)	−49.8058	−72.19455
SV3-16	78.9 ± 2.3	82.2 ± 1.5	0.36	8	83.8 ± 1.0	0.9	17	82.2 ± 1.5	YC1σ(2+)	−49.80524	−72.18593
EA-10	78.7 ± 5.1	82.3 ± 2.6	0.33	7	82.5 ± 2.6	0.51	8	82.3 ± 2.6	YC1σ(2+)	−50.14328	−72.34297
SV1-2	80.3 ± 2.7	83.2 ± 1.7	0.39	8	85.2 ± 1.2	1.06	15	83.2 ± 1.7	YC1σ(2+)	−49.76109	−72.40588
SM-24	90.0 ± 5.7	94.2 ± 1.3	0.29	18	95.0 ± 1.7	1.6	19	94.2 ± 1.3	YC1σ(2+)	−49.47496	−72.49262
EP-2	91.4 ± 3.0	94.2 ± 2.4	0.29	12	95.6 ± 2.2	0.8	14	94.2 ± 2.4	YC1σ(2+)	−50.12853	−72.18836

are simplified by abundant and areally extensive exposures of the contact between the shallow-marine La Anita Formation and the terrestrial Cerro Fortaleza Formation, as well as an apparent lack of significant structural complication (Fig. 8). Eastward from the Rio Leona area (Fig. 5a), the Cerro Fortaleza Formation is traceable another 30 km E-ENE to the VL-1 sample locality (Fig. 5a). Beyond this area, direct correlation of the unit to the east is hindered by the presence of extensive Cenozoic flood basalt. However, lithofacies-equivalent rocks that are exposed 30 km further NE near the town of Tres Lagos have been identified by previous workers as a continuation of the Cerro Fortaleza Formation (the Mata Amarilla Formation of Goin *et al.*, 2002; Varela *et al.*, 2012a).

In the area north of Lago Viedma, precise correlations are difficult due to the lack of detailed definition in the stratigraphy. We outline here a proposed cross-section for the area based on field observations, published subsurface data and in part by DZ MDAs that are discussed below (Fig. 9a). In our proposed cross-section (Fig. 9a), we suggest that the upper Cretaceous (Cenomanian to Coniacian) shallow-marine deposits of the undifferentiated Lago Viedma and Puesto El Alamo Formations dip eastward in to the subsurface in the vicinity of sample SM-24. Dip into the subsurface is observable in the field (see Appendix S2 for a detailed discussion). Stratigraphy to the east of this appears to be relatively flat lying and consists of poorly described shallow-marine and terrestrial deposits that must be younger than what we define as undifferentiated Lago Viedma and Puesto El Alamo (abbreviated unit Kpelv), based on the law of stratigraphic superposition.

Previously published E-W oriented cross-sections through this area have employed an east-vergent blind thrust to bring Cenomanian stratigraphy back to the surface to the east of the study area (e.g. Giacosa *et al.*, 2012; Fig. 8b). Our proposed cross-section for the same area does not include this blind thrust or any significant reappearance of Cenomanian stratigraphy at the surface to the east (Fig. 8a). We propose this configuration for three reasons: (1) unit Kpelv is observed dipping into the subsurface in the vicinity of sample SM-24 (Figs 5 and 8c) with no obvious surface expression of a structure that might bring the unit back to the surface; (2) subsurface data show the Middle Inoceramus seismic unit, which represents phase 2 stratigraphy of Cenomanian to Coniacian age in the subsurface, to be between 300 m and 1100 m below the land surface in the study area (Sachse *et al.*, 2015; Fig. 9c); and (3) new DZ MDAs from this study show that terrestrial strata that were previously assigned a Cenomanian age are likely younger than Cenomanian. This new cross-section suggests that the rocks located east of Lago Viedma are dominantly younger than Coniacian except where local structures might expose

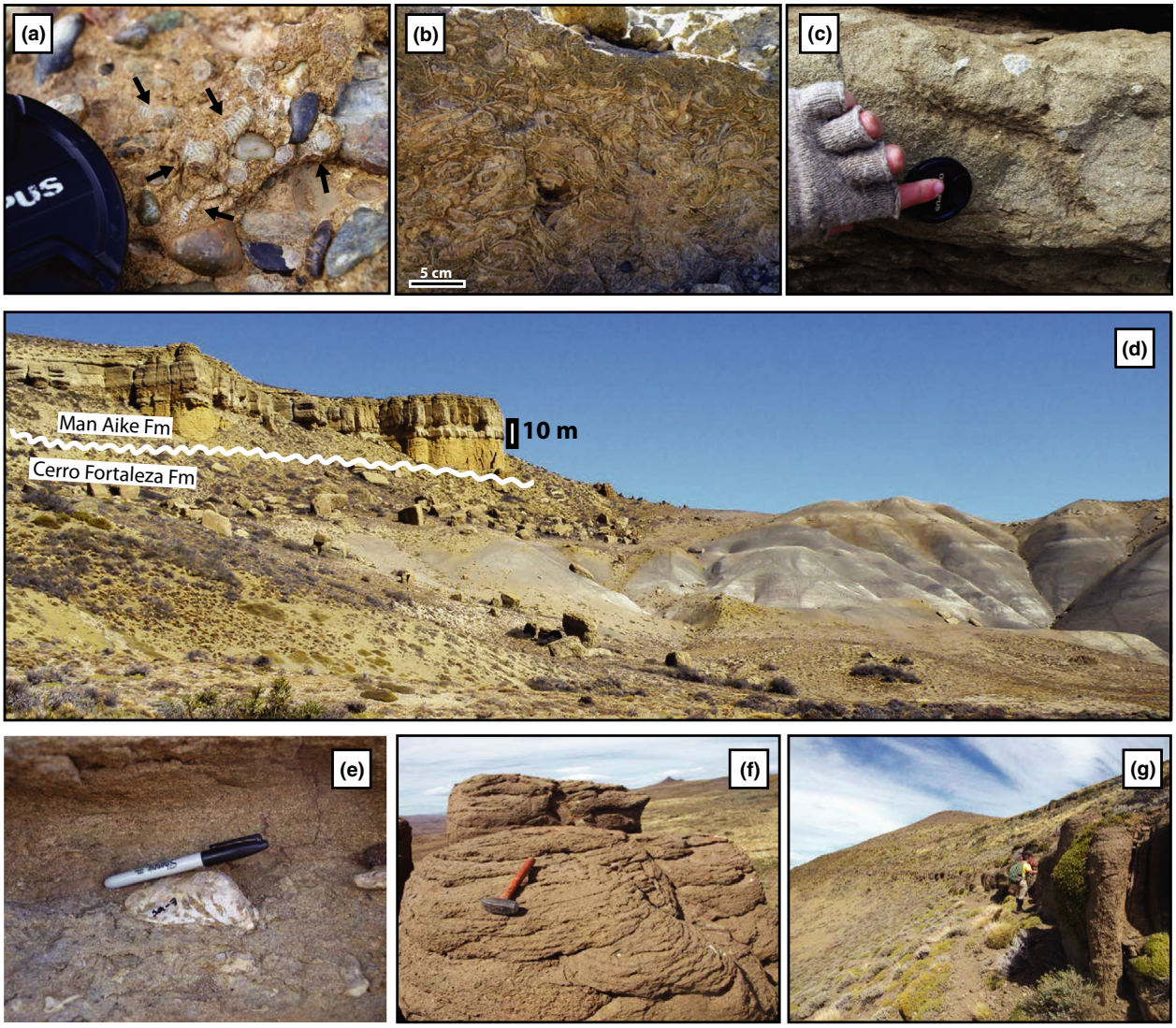

Fig. 7. Field photos of features within Cenozoic phase 3 strata. (a) Coral fragments (black arrows) in a conglomerate in the Man Aike Formation; camera lens for scale. (b) Oyster fragment 'hash' in the Man Aike Formation. (c) *Ophiomorpha* in the Man Aike Formation; camera lens for scale. (d) Overview of the unconformable relationship between the Cerro Fortaleza Formation and the Eocene Man Aike Formation at the geographic locality Cerro Fortaleza (Fig. 5). (e) Oyster in the Cangrejo Sandstone; pen is 15 cm long. (f) Large-scale trough cross-stratification in the Cangrejo Sandstone; hammer is 30 cm long. (g) Overview photo of the limited exposure of the Cangrejo Sandstone in the Rio Cangrejo Valley; person for scale.

small windows of older stratigraphy (see Appendix S2 for a complete discussion of this cross-section).

New detrital zircon MDAs

Samples SV1-2 (YC1σ: 83.2 ± 1.7 Ma; Table 1; Figs 5a, c and 10) and EA-10 (YC1σ: 82.3 ± 2.6 Ma; Table 1; Figs 5a, c and 10) provide a maximum age for the transition from shallow-marine to terrestrial deposition in the western part of the study area (see Tables S1 and S2 for full U-Pb data tables for all samples). These samples are from the uppermost La Anita Formation and show the transition to be Campanian at oldest. Samples throughout the terrestrial Cerro Fortaleza Formation in this area show maximum depositional ages that are Campanian, with the stratigraphically highest sample EP-13 providing a YC1σ MDA of 76.2 ± 1.6 Ma (Figs 5a, c and 10). The La Anita Formation is not exposed east of Rio Leona throughout most of the study area. Sample VL-1 (YC1σ: 82.1 ± 2.4 Ma; Table 1; Figs 5a, c and 10) from stratigraphy defined as 'lower Mata Amarilla' by Varela (2015) provides a maximum depositional age for the lower part of terrestrial deposits in the eastern part of the study area.

Table 2. Summary of the measured thickness of the Cerro Fortaleza Formation compiled from this study and Varela (2015). Coordinates are in WGS84.

	Cerro Fortaleza Formation thickness				
Figure 4	Longitude	Latitude	Thickness (m)	Type	Source
1	−72.233204	−49.868010	575	Estimated full	This study
2	−72.189814	−49.804336	439	Measured minimum	This study
3	−72.238750	−50.056680	215	Measured minimum	This study
4	−72.026633	−49.941113	350	Measured minimum	Varela (2015)
5	−71.661310	−49.894729	185	Measured minimum	Varela (2015)

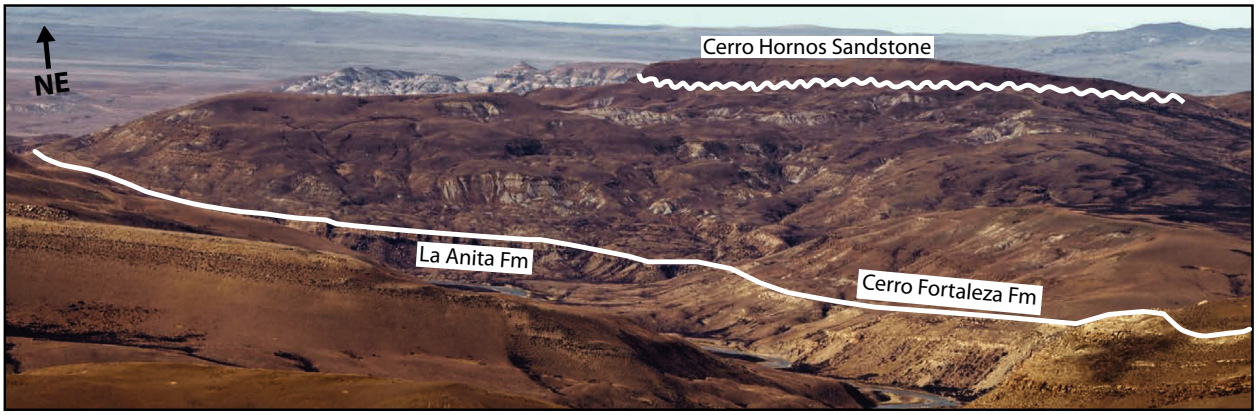

Fig. 8. Field photo overview illustrating the relatively uncomplicated stratigraphic relationships in the field area. Photo was taken looking NE from near location 1 on Fig. 5.

Samples from phase 3 stratigraphy above the unconformity in this area show that the Man Aike Formation has a YSG MDA of 43.3 ± 2.0 Ma (sample CF-1C; Fig. 5). Although this MDA is not as robust as those from underlying phase 2 stratigraphy, and Man Aike sample EP-21 does not suggest an Eocene age, Macellari *et al.* (1989) identified the Palaeogene bivalve *Venericardia* at the same localities sampled for DZ in this study and correlated the unit to Eocene Man Aike Formation to the south. In addition, a YC1σ MDA of 26.2 ± 1.5 Ma from sample ZC-14 above the unconformity at Cerro Hornos suggests that earliest phase 3 deposits in this area are not Man Aike Formation. The late Oligocene MDA suggests that this is a previously unrecognized and unnamed unit. We propose the informal name 'Cerro Hornos Sandtsone' until such time as this unit can be formally defined.

Sample SM-24 from the shallow-marine deposits of the undifferentiated Lago Viedma and Puesto El Alamo Formation shows a Cenomanian YC1σ MDA of 94.2 ± 1.3 Ma (Table 1; Fig. 5a, c). This is consistent with Cenomanian MDAs for equivalent stratigraphy to the west, calculated from the data of Malkowski *et al.* (2017; Fig. 2). A YC1σ MDA of 18.1 ± 0.3 Ma from sample SM-9 in the Rio Cangrejo Valley shows, for the first time, that there are Cenozoic strata preserved on this side of Lago Viedma. Similar to the Cenozoic stratigraphy at Cerro Hornos, this unit is previously unrecognized and unnamed. We propose the informal name 'Cangrejo Sandstone' for this unit until such time as it can be formally defined.

Detrital zircon provenance

Detrital zircon provenance signatures of the Upper La Anita and Cerro Fortaleza Formations, as well as overlying Cenozoic strata, are consistent with derivation from known source regions for the upper Cretaceous MAB basin fill (Fig. 11; e.g. Malkowski *et al.*, 2017). All samples contain age peaks representative of zircon derived from the Eastern Andean Metamorphic Complex basement terrane (EAMC, 200–3500 Ma; Fig. 11), Chon Aike volcanic province (145–200 Ma; e.g. Pankhurst *et al.*, 2000; Malkowski *et al.*, 2015b) and the Patagonia Batholith (25–144 Ma; e.g. Hervé *et al.*, 2007). Phase 3 Cenozoic units may have also received recycled sediment from uplifted phase 2 Cretaceous sediments that were cannibalized in the evolving southern Andean fold and thrust belt (e.g. Fosdick *et al.*, 2014).

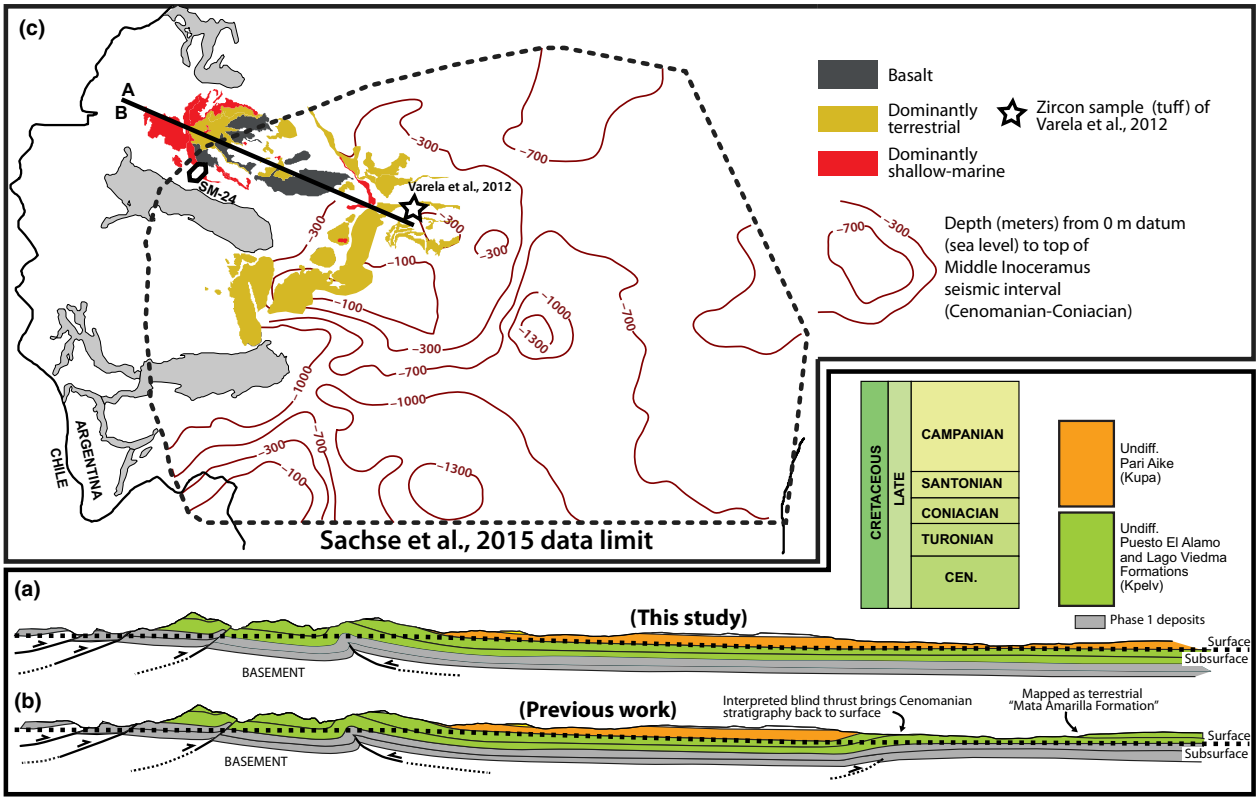

Fig. 9. Schematic cross-sections for the stratigraphy on the north shore of Lago Viemda and summary of evidence that Cenomanian stratigraphy is in the subsurface in the eastern part of the study area. (a) Proposed cross-section presented in this study based on field relationships and new DZ MDAs. (b) Previously published cross-section from Giacosa *et al.* (2012) showing a blind thrust bringing Cenomanian stratigraphy back to the surface in the eastern part of the study area. (c) Geologic mapping and sample locations superimposed on a depth to surface contour map from Sachse *et al.* (2015) showing their interpreted top of the Cenomanian–Coniacian seismic unit 'Middle Inoceramus'. Note that the minimum land surface elevation in this area is approximately 200 m above sea level suggesting that Cenomanian–Coniacian stratigraphy should be at least 300 m below land surface across the study area (see Appendix S2 for a more detailed discussion).

DISCUSSION

Refined stratigraphic framework of the austral sector

Extensional history (phase 1)

The extensional history of the Austral sector was described by Malkowski *et al.* (2015b) and Ramos *et al.* (1982). Both studies focused on the geochemistry and geochronology of this phase, which lasted in the MAB from approximately 154 Ma to 115 Ma (Ghiglione *et al.*, 2015; Malkowski *et al.*, 2015a). A detailed description of the sedimentary fill of the RVB in the Austral sector can be found in Arbe (2002).

Initiation of foreland sedimentation (phase 2)

Previously published U-Pb geochronology suggests that the foreland phase of the MAB initiated between 115 Ma and 100 Ma in the northernmost Austral sector (Ghiglione *et al.*, 2015; Malkowski *et al.*, 2015a,b). This initial foreland phase is recorded in the northernmost part of the basin (47.5° S) by shallow marine to deltaic facies (Ghiglione *et al.*, 2015) that transition southward into deep-marine facies (Figs 2 and 3a; Malkowski *et al.*, 2015b). This transition may occur as far north as 49.3° S, but is definitive at 49.7° S. Radiometric age controls support the original model for the depositional history of the MAB, or what we refer to as the deep-marine model. The new Campanian–Maastrichtian age for Austral terrestrial deposits in the study area, defined by multiple maximum depositional ages, directly contradicts the Cenomanian age assigned by Varela *et al.* (2012a,b) based on a single tuff age. Therefore, the terrestrial deposits likely do not represent initial phase 2 sedimentation.

We suggest that the Cenomanian tuff age of Varela *et al.* (2012a,b) is not viable for the terrestrial deposits of the eastern part of the Austral outcrop belt for three reasons: (1) new DZ MDAs from this study for the same unit suggest that these deposits cannot be older than Campanian (Figs 5 and 10); (2) subsurface data suggest that the top of the Middle Inoceramus interval, the seismic unit that

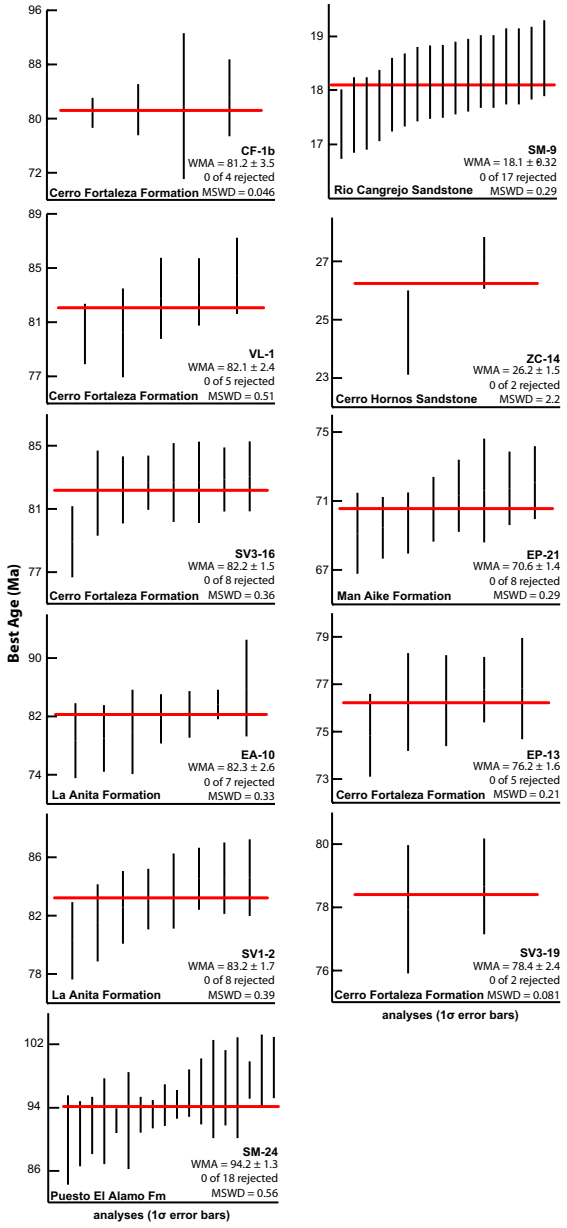

Fig. 10. Calculated YC1σ MDAs for all new detrital zircon samples presented in this study (excludes samples CF-1C from the Man Aike Formation for which we employ a YSG MDA and sample EP-2 from the La Irene Sandstone which produced an MDA approximately 15 Myr older than surrounding stratigraphy and is therefore not considered useful for stratigraphic interpretations in this study) WMA: weighted mean average; MSWD: mean squared weighted deviation.

encompasses Cenomanian to Coniacian MAB stratigraphy, sits between 300 m and 1100 m below land surface within the study area (Sachse *et al.*, 2015; see Appendix S2 for complete discussion); and (3) DZ (this study) and petrographic (Varela *et al.*, 2013) provenance data, coupled with dominantly east- to southeast-directed palaeocurrents (Varela *et al.*, 2013), suggest that the terrestrial deposits were derived from material that was transported away from the southern Andean orogen, located to the west. The presence of Cenomanian deep-marine facies between the terrestrial deposits in question and the southern Andes would omit the opportunity for fluvial systems to drain the arc eastward across a deep-marine foredeep at this time (e.g. Malkowski *et al.*, 2015b). Based on these lines of evidence, we consider the Campanian to Maastrichtian age suggested by DZ MDAs for these deposits to be broadly applicable for terrestrial deposits near Tres Lagos and the north shore of Lago Viedma. With the consideration that rocks are generally older in the northern part of this basin, this age range may approach Santonian to Coniacian moving north, but likely does not approach Cenomanian anywhere in the study area that is outlined in Fig. 5 (see Appendices for more detailed discussion). Additionally, deposits called Campanian La Anita Formation in many publications employing fluvial model stratigraphy are often mismapped entirely (e.g. Fig. 5; Varela *et al.*, 2012a,b, 2013; Varela, 2015). This stratigraphy is in fact Cenozoic in age as demonstrated by our new DZ MDAs (Figs 5 and 10).

Late cretaceous cessation of marine deposition (phase 2)

The Late Cretaceous shoaling of the Austral sector was first comprehensively described by Macellari *et al.* (1989), who provided a framework for the Campanian and younger Austral stratigraphy. Those authors suggested a late Campanian age for the transition from the deep-marine Alta Vista Formation through the shallow-marine La Anita Formation and into the terrestrial Cerro Fortaleza Formation. Subsequent work by Arbe (2002) suggested a transition age of 85 Ma. Our DZ MDAs from the Cerro Fortaleza and La Anita Formations from this study agree with these age assignments, although Arbe's (2002) age assignment is likely slightly too old. There is, however, a small but significant difference between those previously published frameworks and what we interpret here. Macellari *et al.* (1989) and Arbe (2002) suggested an almost exclusively inter-fingering relationship between the Cerro Fortaleza and La Anita Formations in a north–south direction (e.g. Fig. 12). Such a relationship suggests that the shallow-marine deposits of the La Anita Formation are not present along the southern shore of Lago Viedma, and was explained from a sequence stratigraphy perspective by placing a sequence boundary at the base of the Cerro Fortaleza/La Anita system. Mapping from this study shows that the La Anita Formation underlies the Cerro Fortaleza Formation across the study area, although the unit does appear to thin to the north and the entire shoaling upward sequence is broadly gradational (Fig. 12). The presence of dinosaur bones throughout the terrestrial portions of this section in the Austral sector (e.g. Novas *et al.*, 2013; Lacovara *et al.*, 2014) suggests that this phase of the basin did not last past the end of the

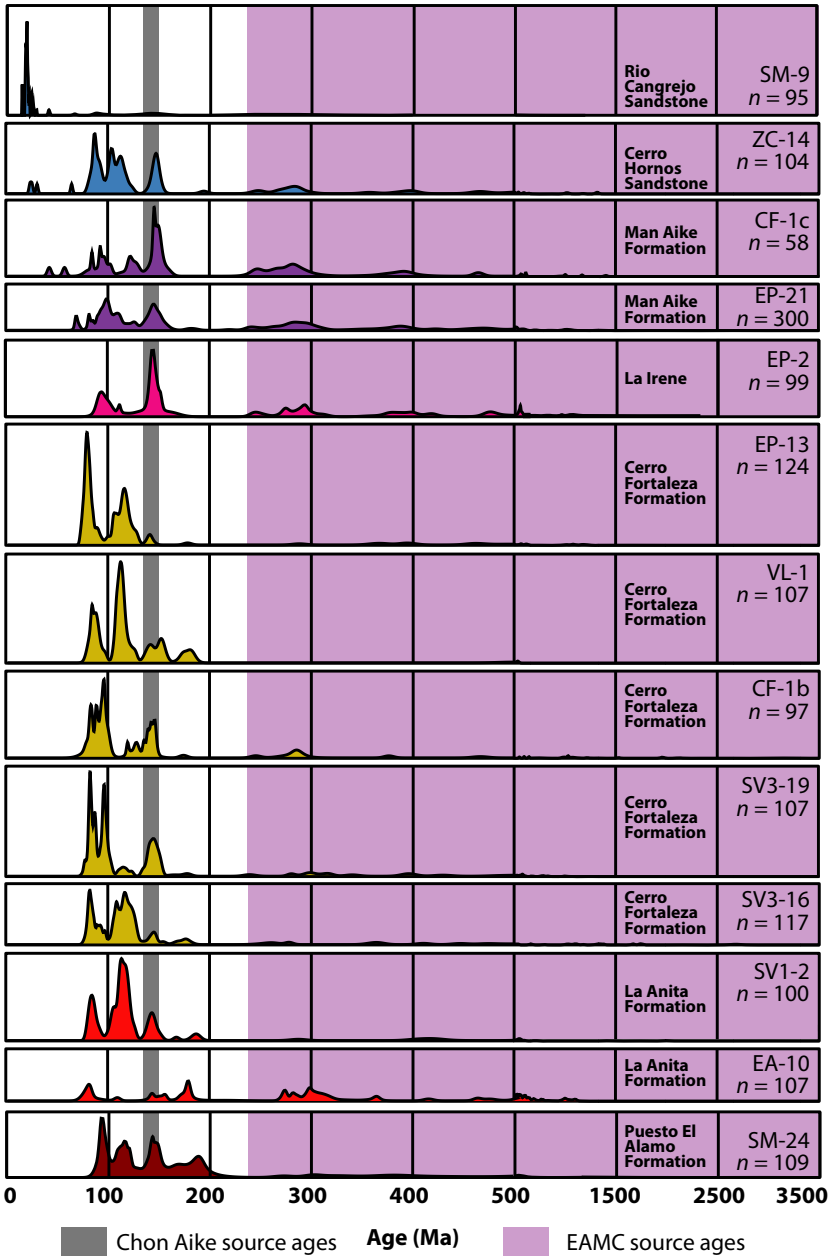

Fig. 11. Probability density plots (PDPs) of the U-Pb age distributions for all samples. Colour scheme of PDP curves follows that of Fig. 5.

Cretaceous or if it did, the Palaeogene unconformity has removed that record.

Palaeogene unconformity (phase 3)

Malumiàn *et al.* (2000) identified a regional Palaeogene unconformity that exists in both the Austral and Magallanes sectors of the foreland basin system (Fig. 13). Based on new DZ ages, the magnitude of the unconformity that separates Cretaceous from Cenozoic strata varies across the basin, possibly by more than 40 Myr (Fig. 13). In the southeastern part of the study area (Fig. 5), the unconformity places shallow marine rocks of probable Eocene age (Man Aike Formation) on Campanian to Maastrichtian rocks (Cerro Fortaleza Formation). This overlying unit contains facies and faunal assemblages that are similar to the Man Aike Formation from the Magallanes sector 'Calafate Formation' of Macellari *et al.*, 1989), suggesting at least 20 Myr of missing time. The same configuration is present in the Magallanes sector, where the Eocene Man Aike Formation sits on the uppermost phase 2 deposits, the Maastrichtian Dorotea Formation (Fig. 13;

Schwartz & Graham, 2015). To the north, the age of the stratigraphy overlying the Cerro Fortaleza Formation decreases substantially (Figs 5 and 13). Just south of Rio Guanaco near location 1 (Fig. 5), the stratigraphy overlying the Cerro Fortaleza Formation is upper Oligocene or younger. This unit has very limited exposure at the top of two mesas and has no formally assigned name, but suggests at least 40 Myr of missing time. To the north, sample SM-9 (Fig. 5) represents the first evidence that this unconformity is preserved north of Lago Viedma. This sample is from a previously unmapped unit in the Cangrejo River Valley. Although the sample provides a robust MDA of 18.1 $\pm$ 0.32 Ma (YC1σ), the exact relationship between this unit and the underlying stratigraphy remains unknown. Further mapping and geochronology are required to elucidate the full nature of the unconformity this far north, but the early Miocene MDA of SM-9 and the general trend of Cretaceous foreland deposits getting older to the north suggest as much as 60 Myr of missing time (Fig. 13).

The lateral variation in magnitude of the unconformity highlights the complexity of its origin and/or the post-unconformity depositional history within the study area. Similarly, the age range of the unconformity in the Magallanes sector of the basin varies (Malumiàn *et al.*, 2000; Schwartz *et al.*, 2012; Ali & Fosdick, 2015; Fosdick *et al.*, 2015). Altogether, the presence of the unconformity throughout the basin system reveals a regional, basinwide tectonic and erosional event. However, lateral variation in the magnitude of the unconformity, as well as the nature of the deposits that overlie the horizon, indicates a non-uniform episode of erosion and non-uniform sedimentation following the erosional event.

IMPLICATIONS OF THE REFINED FRAMEWORK

Basement architecture

The abrupt and drastic transitions in the flexural rigidity of the MAB basement that are required to explain the fluvial model framework are unnecessary with the reassignment of the age of Austral sector terrestrial deposits (Figs 4 and 13). The evidence for the hypothesized abrupt transitions in lithospheric flexural rigidity of the fluvial model was the close proximity of terrestrial and deep-marine deposits of the same age (Cenomanian). This close proximity was interpreted to be a function of abrupt discontinuities in flexural rigidity of underlying basement (e.g. Fig. 4). Our redefinition of the age of the terrestrial deposits in question from Cenomanian–Santonian to Campanian–Maastrichtian demonstrates that these deposits are not age equivalent to nearby deep-marine stratigraphy, and thus eliminates the need to explain terrestrial deposition in very close proximity to deep-marine deposition. The refined framework based on a Campanian–Maastrichtian age is consistent with a broad, gradual transition from south to north in the flexural rigidity of the basement that was inherited from the early rift phase 1 of the basin (Fig. 13). This is not to say, however, that some inherited characteristics may not influence more local depositional trends through parts of the basin.

This interpretation is conceptually built on the initial south to north 'unzipping' of the MAB described by Ramos *et al.* (1982) and Malkowski *et al.* (2015b) who suggest the degree of lithospheric attenuation decreases to the north. This would be consistent with a northward increase in elastic thickness of the lithosphere and associated flexural rigidity and decreased flexural subsidence during foreland phases. This explanation remains largely conceptual as detailed seismic imaging of MAB basement is not available for the northern part of the basin and this basin configuration has not been explicitly modelled.

Provenance of Campanian and younger deposits

Although the DZ age distributions in all samples are consistent with known source regions to the west of the basin in the arc and fold and thrust belt, temporal trends in the proportions of age populations suggest tectonic reconfiguration within the source region through time. From the Campanian(?) La Anita to Campanian–Maastrichtian(?) Cerro Fortaleza Formations , the proportion of EAMC-derived zircon decreases and Chon Aike and Patagonia batholith-derived zircon increases (Fig. 11).

Correlations with strata in the Magallanes basin

New age constraints from this study allow for tentative geochronology-based correlations with units that are well defined in the Magallanes sector of the basin (approximately 60 km south of the study area; Fig. 13a). The maximum depositional age of 82.3 $\pm$ 2.6 Ma derived from the upper La Anita Formation (EA-10) suggests that the upper La Anita and lower Cerro Fortaleza Formations are at least partly correlative with the deep-marine Tres Pasos Formation (Campanian) and/or the shallow- to marginal-marine Dorotea Formation (Campanian–Maastrichtian; Fig. 13a; Schwartz *et al.*, 2016). Similarly, Eocene zircon grains and fossil assemblages within the Man Aike Formation at Cerro Fortaleza confirm a correlation with the Man Aike Formation that has been mapped in the Rio Baguales area of Chile (Fig. 13a; Schwartz *et al.*, 2012; Gutiérrez *et al.*, 2017). Oligocene zircon grains from Cenozoic rocks on the south shore of Lago Viedma suggest that the unit is possibly correlative with the Rio Leona Formation that is mapped in the Rio Baguales area of Chile (Gutiérrez *et al.*, 2017) and/or the

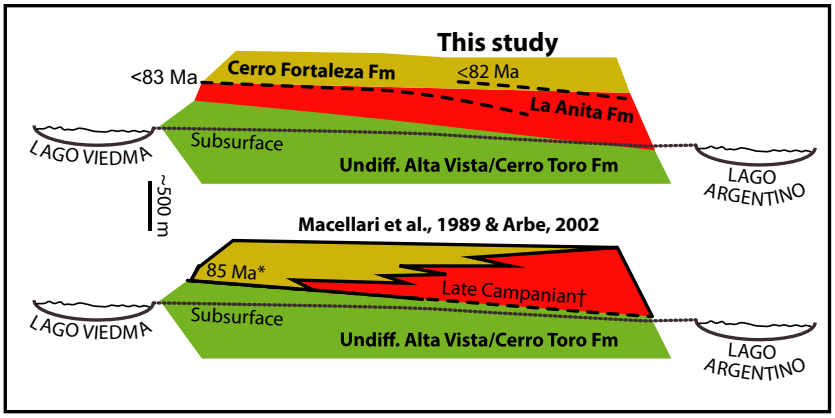

Fig. 12. Comparison of previously interpreted stratigraphic relationships between the La Anita and Cerro Fortaleza Formations and the relationship proposed in this study († age from Macellari *et al.*, 1989; * age from Arbe, 2002).

Rio Turbio Formation that has been mapped on the Chile–Argentina border, 70 km to the south (Fosdick *et al.*, 2015).

Palaeontology

Results from this study suggest that the terrestrial deposits in the Austral sector of the MAB in the vicinity of Lago Viedma and Lago Argentino east to the town of Tres Lagos are no older than Campanian. Therefore, fossils discovered in these deposits should be assigned a Campanian to Maastrichtian age, rather than a Cenomanian age. This reassigns the ages that have been given to several discoveries and alleviates the uncertainty that has been acknowledged for others (e.g. Fig. 5b).

CONCLUSIONS

The tectonic and sedimentary fill history of the MAB can be divided into three distinct phases including a Jurassic extensional phase (phase 1), a Cretaceous foreland basin phase (phase 2) and a Cenozoic foreland basin phase (phase 3). Phase 1 is characterized by diachronous extensional tectonics that generated the back-arc Rocas Verdes Basin (RVB). The RVB was active from at least 154 Ma to approximately 115 Ma, during which extension propagated northward through southern Patagonia (de Wit & Stern, 1981; Ghiglione *et al.*, 2015; Malkowski *et al.*, 2015a,b, 2017). Extension variably attenuated the crust, allowing the formation of oceanic crust in the southern part of the RVB and attenuating continental crust in the north. The extensional back-arc was filled with bimodal volcanic rocks of the El Quemado and Tobífera Formations (de Wit & Stern, 1981; Pankhurst *et al.*, 2000) and black shale of the Rio Mayer and Zapata Formations (Katz, 1963; Wilson, 1991).

Phase 2 includes the transition from extensional to compressional tectonics, the initiation of flexural subsidence and the initiation of foreland sedimentation. The transition into phase 2 was diachronous across the basin, beginning in the northern Austral sector at latitude 47.5° S by *ca.* 115 Ma and propagating southward into the Magallanes sector at latitude 51° S by *ca.* 93 Ma (Fildani *et al.*, 2003; Malkowski *et al.*, 2015a). Phase 2 is recorded by a thick succession of deep-marine deposits that shoal into shallow marine and terrestrial deposits (Romans *et al.*, 2010). New detrital zircon maximum depositional ages (DZ MDAs) from terrestrial strata in the Austral sector that were previously described as Cenomanian (located between 49.5° S and 50.2° S; Fig. 2) suggest that the terrestrial deposits are Campanian or younger. The new ages indicate that the terrestrial deposits represent the upper part of the shoaling-upward succession recorded by phase 2, rather than the initiation of foreland basin sedimentation. These new data, combined with a compilation of previously published U-Pb age dates from igneous and detrital zircon, suggest that the cessation of marine conditions during this phase began prograding southward along the basin during Santonian to Campanian time (Fig. 13).

Phases 2 and 3 are separated by a regional Palaeogene unconformity that spans both the Magallanes and Austral portions of the MAB. New DZ MDAs constrain the age and magnitude of the unconformity, and show that the unconformity is variable in magnitude. The amount of time missing at the unconformity that defines the top of phase 2 stratigraphy increases significantly in the northward direction, representing as little as 20 Myr in the Magallanes sector and as much as 60 Myr in the Austral sector. This unconformity likely represents a record of complex Cenozoic tectonics of the southern Andes and could include multiple tectonic events. Cenozoic deposits of phase 3 that overlie the Palaeogene unconformity are spatially variable in lithology and age.

Using these new age controls and published U-Pb zircon data, we propose a new, basinwide lithostratigraphic and chronostratigraphic framework for the MAB between 49° S and 51.5° S (Fig. 13). This framework is a north–south correlation of deposits in the

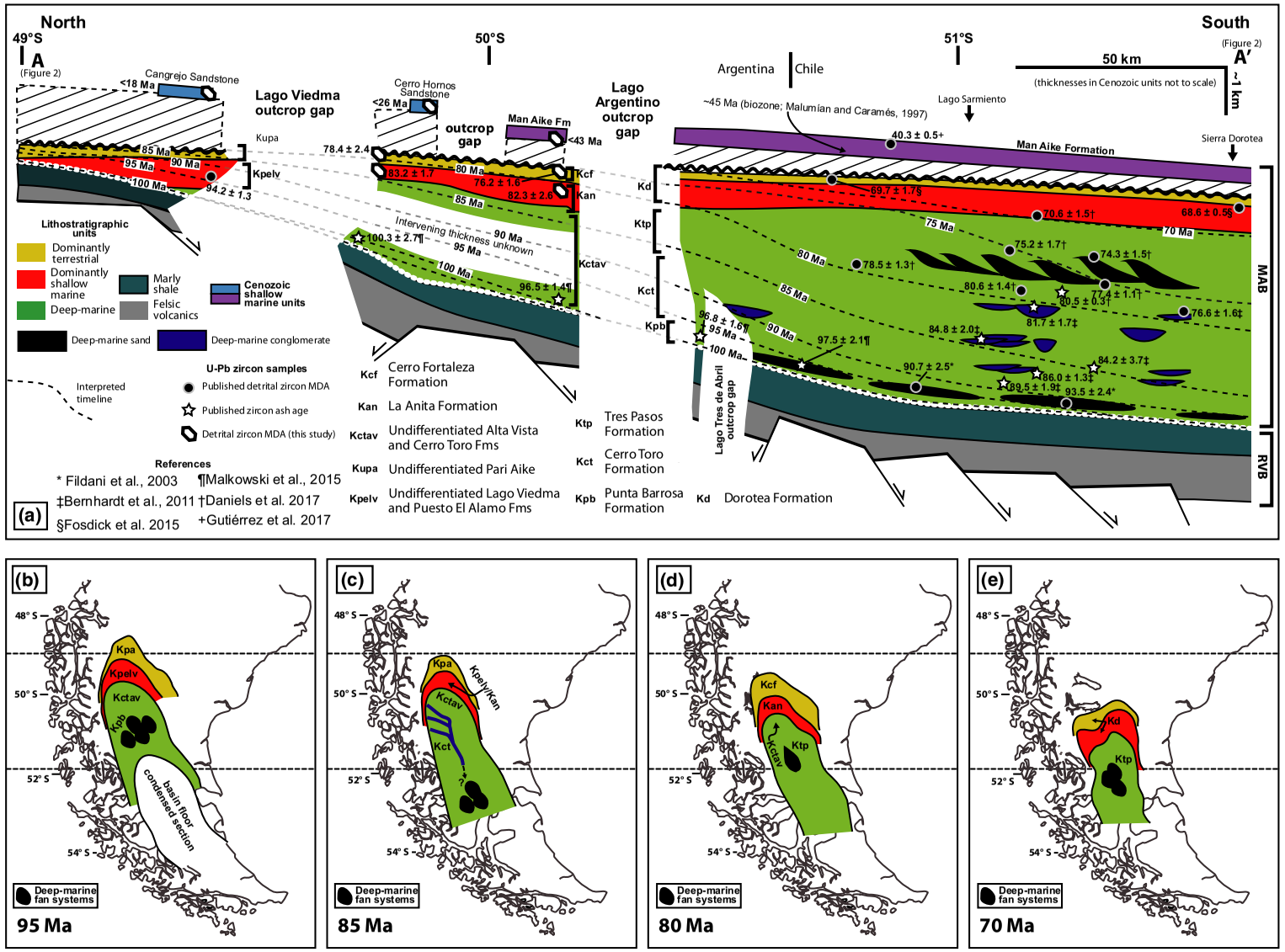

Fig. 13. Refined chronostratigraphic framework and depositional history of the MAB. (a) Composite N-S longitudinal stratigraphic framework of the MAB based on a compilation of new and published U-Pb zircon and ash geochronology data. White dashed line delineates phase 1 stratigraphy from phase 2. (b–e) Schematic palaeogeographic maps of the MAB depositional system. Note the location of the deep-marine to shallow-marine transition seems to have remained around 50° S through the Coniacian (until 85 Ma) after which it takes an abrupt step south and continues to prograde S-SE in to the Maastrichtian. Basin margins are after Biddle *et al.* (1986) and Sachse *et al.* (2015). Depositional systems relationships are based on a compilation of mapping and U-Pb data from this study compiled with previously published interpretations of Wilson (1991) and Arbe (2002) and the previously published mapping and U-Pb data summarized in Figs 2 and 13a.

Austral sector with deposits in the Magallanes sector, and is based on a combination of DZ MDAs, ash ages and biostratigraphy from both basin sectors. Ultimately, the proposed chronostratigraphy (Fig. 13) is the first holistic attempt to correlate the poorly dated stratigraphy of the Austral sector of the MAB with the well-constrained stratigraphy of the Magallanes sector of the MAB. The correlations alleviate the complexities associated with highly variable stratigraphic nomenclature, and refine the ages of units that were previously of unknown and/or of questionable age. The new compilation provides a robust foundation for future basin history studies, and provides a robust chronostratigraphic template for the rich palaeontologic discoveries in Patagonia, including dinosaur faunas.

Finally, our new age constraints and stratigraphic framework affects a number of previously published interpretations that suggest a Cenomanian age for terrestrial stratigraphy in the study area. These studies have examined palaeontology (O'Gorman & Varela, 2010; Griffin & Varela, 2012), tectonic evolution and sediment supply (Varela, 2015), Austral sector provenance (Varela *et al.*, 2013) and palaeoclimatology (Varela *et al.*, 2012b, 2018). The results of this study show that interpretations made based on a Cenomanian age for the terrestrial deposits between Lago Viedma, Lago Argentino and Tres Lagos (Fig. 5) are invalid. Instead, data and non-age-dependent interpretations from these previous studies describe the Campanian to Maastrichtian conditions in the MAB.

ACKNOWLEDGEMENTS

This work was funded by the Stanford Project on Deep-Water Depositional Systems (SPODDS) and the Stanford University Mcgee-Levorsen Grant. Field assistance was provided by G. Sharman, M. Malkowski, A. Reimchen, D. Orme and M. Thomas. We would like to thank the staff members of the Arizona LaserChron Center for their assistance in detrital zircon analysis and data reduction. The Arizona LaserChron Center is funded in part by the National Science Foundation Instrumentation and Facilities Division (NSF Grant NSF-EAR 1338583). Discussions with K. Surpless and D. Orme helped shape this manuscript. Editor N. McQuarrie and reviewers M. Streker, B. Currie, C. Painter and an anonymous reviewer provided reviews that significantly improved this work.

SUPPORTING INFORMATION

Additional Supporting Information may be found in the online version of this article:

Fig S1. Full map of the Magallanes-Austral basin divided by lithostratigraphic units.

Appendix S1. Full descriptions of lithologic units in the Magallanes–Austral basin.

Appendix S2. Selected field relationships.

Table S1. U-Th-Pb isotope composition of detrital zircons analysed at the Arizona Laserchron Center.

Table S2. U-Th-Pb isotope composition of detrital zircons analysed at the University of California Santa Cruz.

REFERENCES

Ali, R. & Fosdick, J.C. (2015) Thermal history of the Maastrichtian-Eocene Magallanes (Austral) foreland basin, Patagonia (50.5-51.5°S): preliminary findings from vitrinite reflectance analysis and detrital zircon thermochronology. AAPG Eastern Section 44th Meeting, Indianapolis, 44, 27.

Arbe, H.A. (2002) Anàlisis estratigràfico del Cretàcico de la Cuenca Austral. In: *Geologià y Recursos Naturales de Santa Cruz* (Ed. by Haller M.J.) *Relatorio del XV Congreso Geológico Argentino, El Calafate*, **8**, 103–128.

Arbe, H.A. & Hechem, J.J. (1984) Estratigrafia y facies de depósitos continentals, litorales, y marinos del Cretàcico superior, lago Argentino, Actas 9 Congreso Geológico Argentino. 124-158.

Benson, R.B.J., Carrano, M.T. & Brussate, S.L. (2010) A new clade of archaic large-bodied predatory dinosaurs (Theropoda: Allosauroidea) that survived to the latest Mesozoic. *Naturwissenschaften*, **97**, 71–78.

Bernhardt, A., Jobe, Z.R., Grove, M. & Lowe, D.R. (2011) Paleogeography and diachronous infill of an ancient deep-marine foreland basin, Upper Cretaceous Cerro Toro Formation, Magallanes Basin. *Basin Res.*, **24**, 269–294.

Biddle, K.T., Uliana, M.A., Mitchum, R.M., Fitzgerald, M.G. & Wright, R.C. (1986) The stratigraphic and structural evolution of the central and eastern Magallanes Basin, southern South America. In: *Foreland Basins* (Ed. by Allen A. & Homewood P.) *Int. Assoc. Sedimentol. Spec. Publ.*, **8**, 41–61.

Caldéron, M., Prades, C.F., Hervé, F., Avendaño, V., Fanning, C.M., Massonne, H.J., Theye, T. & Simonetti, A. (2013) Petrological vestiges of the Late Jurassic-Early Cretaceous transition from rift to back-arc basin in southernmost Chile: new age and geochemical data from the Capitán Aracena, Carlos III, and Tortuga ophiolitic complexes. *Geochem. J.*, **47**, 201–217.

Cawood, A., Hawkesworth, C.J. & Dhuime, B. (2012) Detrital zircon record and tectonic setting. *Geology*, **40**, 875–878.

Dalziel, W.D. (1981) Back-Arc extension in the southern Andes: A review and critical reappraisal. *Philos. Trans. R. Soc. Lond.*, **300**, 319–335.

Daniels, B.G., Auchter, N.C., Hubbard, S.M., Romans, B.W., Matthews, W.A. & Stright, L. (2017) The timing of deep-water slope evolutionary phases constrained by large-n detrital and volcanic ash zircon geochronology, Cretaceous

Magallanes Basin, Chile. *Geol. Soc. Am. Bull.* https://doi.org/10.1130/b31757.1.

Decelles, G. & Giles, K.A. (1996) Foreland basin systems. *Basin Res.*, **8**, 105–123.

Desegaulx, P., Roure, F. & Villein, A. (1990) Structural evolution of the Pyrenees: tectonic inheritance and flexural behavior in the continental crust. *Tectonophysics*, **182**, 211–225.

Dickinson, W.R. & Gehrels, G.E. (2009) Use of U-Pb ages of detrital zircons to infer maximum depositional ages of strata. A test against a Colorado Plateau Mesozoic database. *Earth Planet. Sci. Lett.*, **288**, 115–125.

Egerton, M., Williams, C.J. & Lacovara, K.J. (2016) A new Late Cretaceous (late Campanian to early Maastrichtian) wood flora from southern Patagonia. *Paleogeogr. Paleoclimatol. Paleoecol.*, **441**, 305–316.

Fildani, A., Cope, T.D., Graham, S.A. & Wooden, J.L. (2003) Initiation of the Magallanes foreland basin: timing of the southernmost Patagonian Andes orogeny revised by detrital zircon provenance analysis. *Geology*, **31**, 1081–1084.

Fosdick, J.C., Romans, B.W., Fildani, A., Bernhardt, A., Calderón, M. & Graham, S.A. (2011) Kinematic evolution of the Patagonian retroarc fold-and-thrust belt and Magallanes foreland basin, Chile and Argentina, 51°30′S. *Geol. Soc. Am. Bull.*, **123**, 1679–1698.

Fosdick, J.C., Graham, S.A. & Hilley, G.E. (2014) Influence of attenuated lithosphere and sediment loading on flexure of the deep-water Magallanes retroarc foreland basin, Southern Andes. *Tectonics*, **33**, 2505–2525.

Fosdick, J.C., Grove, M., Graham, S.A., Hourigan, J.K., Lovera, O. & Romans, B.W. (2015) Detrital thermochronologic record of burial heating and sediment recycling in the Magallanes foreland basin, Paragonia Andes. *Basin Res.* https://doi.org/10.1111/bre.12088.

Gehrels, G.E. & Pecha, M. (2014) Detrital zircon U-Pb geochronology and Hf isotope geochemistry of Paleozoic and Triassic passive margin strata of western North America. *Geosphere*, **10**, 49–65.

Gehrels, G.E., Valencia, A. & Ruiz, J. (2008) Enhanced precision, accuracy, efficiency, and spatial resolution of U-Pb ages by laser ablation-multicollector-inductively coupled plasma-mass spectrometry. *Geochem. Geophys. Geosyst.*, **9**. https://doi.org/101.1029/2007gc001805.

Ghiglione, M.C., Likerman, J., Barberón, V., Beatriz Giambiagi, L., Aguirre-Urreta, B. & Suarez, F. (2014) Geodynamic context for the deposition of coarse-grained deep-water axial channel systems in the Patagonian Andes. *Basin Res.*, **26**, 726–745.

Ghiglione, M.C., Naipauer, M., Sue, C., Barberón, V., Valencia, V., Aguirre-Urreta, B. & Ramos, A. (2015) U-Pb zircon ages from the northern Austral basin and their correlation with the Early Cretaceous exhumation and volcanism of Patagonia. *Cretac. Res.*, **55**, 116–128.

Giacosa, R., Fracchia, D. & Heredia, N. (2012) Structure of the southern Patagonian Andes at 49°S, Argentina. *Geol. Acta*, **10**, 265–282.

Goin, F.J., Poiré, D.G., De La Fuente, M.S., Cione, A.L., Novas, F.E., Bellosi, E.S., Ambrosio, A., Ferrer, O., Canessa, N.D., Carloni, A., Ferigolo, J., Ribeiro, A.M., Sales Viana, M.S., Pascual, R., Reguero, M., Vucetich, M.G., Marenssi, S., De Lima Filho, M. & Agostinho, S. (2002) Paleontología y Geología de los sedimentos del Cretácico Superior aflorantes al sur del Río Shehuen (Mata Amarilla, Provincia de Santa Cruz, Argentina). In: Congreso Geológico Argentino, No. 15, Actas: 603-608.

Griffin, M. & Varela, A.N. (2012) Systematic palaeontology and taphonomic significance of the mollusk fauna from the Mata Amarilla Formation (lower Upper Cretaceous), southern Patagonia, Argentina. *Cretac. Res.*, **37**, 164–176.

Gutiérrez, N.M., Le Roux, J.P., Vasquez, A., Carreño, C., Pedroza, V., Araos, J., Oyarzún, J.L., Pino, J.P., Rivera, H.A. & Hinojosa, L.F. (2017) Tectonic events reflected by palaeocurrents, zircon geochronology, and palaeobotany in the Sierra Baguales of Chilean Patagonia. *Tectonophysics*, **695**, 76–99.

Hervé, F., Pankhurst, R.J., Fanning, C.M., Calderón, M. & Yaxley, G.M. (2007) The south Patagonia batholith: 150 my of granite magmatism on a plate margin. *Lithos*, **97**, 373–394.

Katz, H.R. (1963) Revision of cretaceous stratigraphy in Patagonian Cordillera of Ultima Esperanza, Magallanes Province, Chile. *Am. Asso. Petrol. Geol. Bull.*, **47**, 506–524.

Kraemer, E. & Riccardi, A.C. (1997) Estratigrafía de la región comprendida entre los lagos Argentino y Viedma (49° 40′ - 50° 10′ lat. S), Provincia de Santa Cruz. *Revista de la Asociación Geológica Argentina*, **52**, 333–360.

Lacovara, K.J., Lamanna, M.C., Ibiricu, L.M., Poole, J.C., Schroeter, E.R., Ullmann, V., Voegele, K.K., Boles, Z.M., Carter, A.M., Fowler, E.K., Egerton, M., Moyer, A.E., Coughenour, C.L., Schein, J.P., Harris, J.D., Martínez, R.D. & Novas, F.E. (2014) A gigantic, exceptionally complete Titanosaur sauropod dinosaur from southern Patagonia, Argentina. *Sci. Rep.* https://doi.org/10.1038/srep06196.

Macellari, C.E., Barrio, C.A. & Manassero, M.J. (1989) Upper Cretaceous to Paleocene depositional sequences and sandstone petrography of southwestern Patagonia (Argentina and Chile). *J. S. Am. Earth Sci.*, **2**, 223–239.

Malkowski, M.A., Sharman, G.R., Graham, S.A. & Fildani, A. (2015a) Characterization and diachronous initiation of coarse clastic deposition in the Magallanes-Austral foreland basin, Patagonian Andes. *Basin Res.* https://doi.org/10.1111/bre.12150.

Malkowski, M.A., Grove, M. & Graham, S.A. (2015b) Unzipping the Patagonian Andes-Long lived influence of rifting history on foreland basin evolution. *Lithosphere* https://doi.org/10.1130/L489.1.

Malkowski, M.A., Schwartz, T.M., Sharman, G.R., Sickmann, Z.T. & Graham, S.A. (2017) Stratigraphic and provenance variations in the early evolution of the Magallanes-Austral foreland basin: implications for the role of longitudinal versus transverse sediment dispersal during arc-continent collision. *Geol. Soc. Am. Bull.* https://doi.org/10.1130/b31549.1.

Malumiàn, N., Panza, J.L., Parisi, C., Nanez, C., Carames, A. & Torre, A. (2000) Hoja Geologica 5172-III, Yacimiento Rio Turbio (1:125,000). *Serv. Geol. Minero Argentino, Boletin*, **247**, 180.

Martínez, L.C.A., Iglesias, A., Artabe, A.E., Varela, A.N. & Apesteguía, S. (2017) A new Encephalarteae trunk

(Cycadales) from the Cretaceous of Patagonia (Mata Amarilla Formation, Austral Basin), Argentina. *Cretac. Res.*, **72**, 81–94.

Meilan, D. & Maza, A.E. (1994) Mapa Geologico de la Provincia de Santa Cruz Republica Argentina, escala 1:750000, Secretaria de Mineria Direccion Nacional del Servicio Geologico.

Menegazzo, M.C., Catuneanu, O. & Chang, H.K. (2016) The South American retroarc foreland system: the development of the Bauru Basin in the back-bulge province. *Mar. Pet. Geol.*, **73**, 131–156.

Natland, M.L., Gonzales, E.P., Cañon, A. & Ernst, M. (1974) A system of stages for correlation of Magallanes Basin sediments. *Geol. Soc. Am. Mem.*, **139**, 1–73.

Novas, F.E., Ezcurra, M.D. & Lecuona, A. (2008a) *Orkoraptor burkei* nov. gen. et sp., a large theropod from the Maastrichtian Pari Aike Formation, southern Patagonia, Argentina. *Cretac. Res.*, **29**, 468–480.

Novas, F.E., Agnolín, F.L., Ezcurra, M.D., Porfiri, J. & Canale, J.I. (2013) Evolution of the carnivorous dinosaurs during the Cretaceous: the evidence from Patagonia. *Cretac. Res.*, **45**, 174–215.

O'Gorman, J.P. & Varela, A.N. (2010) The oldest lower Upper Cretaceous plesiosaurs (Reptilia, Sauropterygia) from southern Patagonia, Argentina. *Ameghiniana*, **47**, 447–459.

Pankhurst, R.J., Riley, T.R., Fanning, C.M. & Kelley, S.P. (2000) Episodic silicic volcanism in Patagonia and the Antarctic peninsula: chronology of magmatism associated with the break-up of Gondwana. *J. Petrol.*, **41**, 605–625.

Ramos, A., Niemeyer, H., Skarmeta, J. & Muñoz, J. (1982) Magmatic evolution of the Austral Patagonian Andes. *Earth Sci. Rev.*, **18**, 411–443.

Riccardi, A.C. & Aguirre-Uretta, M.B. (1988) Bioestratigrafia del Cenomaniano-Santoniano en la Patagonia Argentina. *Quinto Congr. Geol. Chile. Actas*, **2**, 375–394.

Riccardi, A.C. & Rolleri, E.O. (1980) Cordillera Patagónica Austral. In: *Segundo Simposio de Geología Regional Argentina*, Vo. 2 (Ed. by J.C. Turner), pp. 1163–1306. Segundo Simposio de Geología Regional Argentina, Cordoba, Argentine.

Romans, B.W., Fildani, A., Graham, S.A., Hubbard, S.M. & Covault, J.A. (2010) Importance of predecessor basin history on the sedimentary fill of a retroarc foreland basin: provenance analysis of the Cretaceous Magallanes basin, Chile (50-52°S). *Basin Res.*, **22**, 640–658.

Sachse, F., Strozyk, F., Anka, Z., Rodriguez, J.F. & Di Primio, R. (2015) The tectono-stratigraphic evolution of the Austral Basin and adjacent areas against the background of Andean tectonics, southern Argentina, South America. *Basin Res.* https://doi.org/10.1111/bre.12118.

Schroeter, E.R., Egerton, M., Ibiricu, L.M. & Lacovara, K.J. (2014) Lamniform shark teeth from the late Cretaceous of southernmost South America (Santa Cruz Province, Argentina). *PLoS ONE*, **9**, 1–7.

Schwartz, T.M. & Graham, S.A. (2015) Stratigraphic architecture of a tide-influenced shelf-edge delta. Upper Cretaceous Dorotea Formation, Magallanes-Austral Basin, Patagonia. *Sedimentology*, **62**, 1039–1077.

Schwartz, T.M., Malkowski, M.A. & Graham, S.A. (2012) Evaluation of the close-out of deep-marine deposition in the Magallanes-Austral basin, Patagonian Chile and Argentina. AAPG Search and Discovery Article #90142.

Schwartz, T.M., Fosdick, J.C. & Graham, S.A. (2016) Using detrital zircon U-Pb ages to calculate Late Cretaceous sedimentation rates in the Magallanes-Austral basin, Patagonia. *Basin Res.*, **29**, 725–746.

Sharman, G.R., Graham, S.A., Grove, M. & Hourigan, J.K. (2013) A reappraisal of the early slip history of the San Andreas fault, central California, USA. *Geology*, **41**, 727–730.

Stern, C.R. & De Wit, M.J. (2003) Rocas Verdes ophiolites, southernmost South America: remnants of progressive stages of development of oceanic-type crust in a continental margin back-arc basin. In: *Ophiolites in Earth History* (Ed. by Dilek Y. & Robinson R.T.) *Geol. Soc. Lond. Spec. Publ.*, **218**, 665–683.

Varela, A.N. (2015) Tectonic control of accommodation space and sediment supply within the Mata Amarilla Formation (lower Upper Cretaceous) Patagonia, Argentina. *Sedimentology*, **62**, 867–896.

Varela, A.N., Poiré, D.G., Martin, T., Gerdes, A., Goin, F.J., Gelfo, J.N. & Hoffmann, S. (2012a) U-Pb zircon constraints on the age of the Cretaceous Mata Amarilla Formation, southern Patagonia, Argentina: its relationship with the evolution of the Austral Basin. *Andean Geol.*, **39**, 359–379.

Varela, A.N., Veiga, G.D. & Poiré, D.G. (2012b) Sequence stratigraphic analysis of Cenomanian greenhouse palaeosols: a case study from southern Patagonia, Argentina. *Sed. Geol.*, **67**, 271–272.

Varela, A.N., Gómez-Peral, L.E., Richiano, S. & Poiré, D.G. (2013) Distinguishing similar volcanic source areas from an integrated provenance analysis: implications for foreland Andean basins. *J. Sediment. Res.*, **83**, 258–276.

Varela, A.N., Raigemborn, M.S., Richiano, S., White, T., Poiré, D.G. & Lizzoli, S. (2018) Late Cretaceous paleosols as paleoclimate proxies of high-latitude Southern Hemisphere: Mata Amarilla Formation, Patagonia, Argentina. *Sed. Geol.*, **363**, 83–95.

Waschbusch, P.J. & Royden, L.H. (1992) Spatial and temporal evolution of foredeep basins: lateral strength variations and inelastic yielding in continental lithosphere. *Basin Res.*, **4**, 179–196.

Wilson, T.J. (1991) Transition from back-arc to foreland basin development in the southernmost Andes: stratigraphic record from the Ultima Esperanza District, Chile. *Geol. Soc. Am. Bull.*, **103**, 98–111.

de Wit, M.J. & Stern, C.R. (1981) Variations in the degree of crustal extension during the formation of a back-arc basin. *Tectonophysics*, **72**, 229–260.

Manuscript received 18 March 2107; In revised form 15 November 2017; Manuscript accepted 17 November 2017.